Engineering PEGylated Antibody Fragments for Enhanced Properties and Cancer Detection

Undergraduate Honors Research Thesis

Presented in partial fulfillment of the requirements for graduation *with honors research distinction* in Biochemistry in the undergraduate colleges of The Ohio State University

by

Shubham Mangla

The Ohio State University

May 2016

Oral Examination Committee:

Dr. Thomas J. Magliery, project advisor

Dr. Dmitri Kudryashov

Dr. Edward W. Martin Jr.

Abstract

3E8 is an antibody that targets Sialyl-Tn, a glycan found exclusively on a subset of cancers called adenocarcinomas. This antibody is particularly interesting to the Magliery Lab because of its use in radioimmunoguided surgery, a modern cancer-detecting technique that allows surgeons to intraoperatively visualize and fully resect diseased tissue. Studies have shown that patient outcome is directly correlated to the surgeon's ability to entirely remove the tumor; unfortunately, current full-length antibodies, like 3E8 have long serum lifetimes and poor affinity to Siayl-Tn.

Consequently, we have engineered a smaller version of 3E8 called 3E8.scFv, an antibody fragment with a tunable serum half-life and affinity and stability nearly equal to full length antibodies. Previous studies have shown that the lifetime of 3E8.scFv can be optimized by attaching polyethylene glycol chains (PEGs) to the antibody, but not without decreasing its ability to bind to Sialyl-Tn. These PEGs, which react non-specifically with surface lysine residues on the fragment, may be responsible for the decrease in affinity of 3E8.scFv as they block the binding site. To determine which lysines are potentially problematic, variants of 3E8.scFv that contain mutations to selected lysines will be engineered. These variants will be characterized and studied using a variety of techniques to locate a more stable form of 3E8.scFv that can be non-specifically PEGylated.

In contrast to non-specific PEGylation at lysines, the specific PEGylation of 3E8.scFv.Cys (3E8.scFv with a C-terminal cysteine) will be studied. A variety of techniques, including gel filtration, surface plasmon resonance, differential scanning fluorimetry, and analytical ultracentrifugation will help investigate the biophysical effects of singly PEGylating 3E8.scFv.Cys with a PEGs of different shapes and sizes. The ultimate goal of

this project is to create a stable single chain variable fragment with a completely tunable serum half-life by PEGylation (non-specifically or specifically) for use in radioimmunoguided surgery and imaging.

In addition to its use in vivo, 3E8.scFv can be used in pathology labs to help detect and diagnose adenocarcinomas. The Magliery lab has engineered a variant of 3E8.scFv called 3E8.scFv.FLAG that contains a C-terminal FLAG tag for immunohistochemistry. Numerous chemistries involving this antibody will be tested and analyzed to develop a sensitive and reliable technique for staining adenocarcinomas.

Acknowledgements

Dr. Thomas J. Magliery*, project advisor

Dr. Edward W. Martin, Jr.**, oral exam committee

Dr. Dmitri Kudryashov*, oral exam committee

Dr. Brandon J. Sullivan*, research scientist

Nicholas E. Long***, graduate student

Mengxuan Jia and Jikang Wu***, graduate students (Wysocki Lab)

Dr. Charles L. Hitchcock**, pathologist

Kristin M. Miller**, lead clinical lab technologist

Dr. Kiran Doddapaneni*, postdoctoral researcher

Srividya Murali* and Kimberly Stephany*, research assistants

* The Ohio State University Department of Chemistry and Biochemistry

** The Ohio State University Wexner Medical Center

*** The Ohio State University Biochemistry Program

Funding:

OSU Office of Undergraduate Education Summer Research Fellowship

OSU College of Arts and Sciences Undergraduate Research Scholarship

Enlyton Ltd.

Ohio Third Frontier

Small Business Innovation Research (SBIR) program

Vita

June 2012 ..... North Olmsted High School

May 2016 ..... Candidate for B.S. in Biochemistry, The Ohio State University

Field of Study

Major Field: Biochemistry

Table of Contents

List of Tables

List of Figures

Chapter 1: Introduction

1.1 Radioimmunoguided Surgery (RIGS)

In light of the 1,658,370 new cancer cases predicted by the American Cancer Society for 2015, a large focus of cancer research has been on developing surgical techniques to effectively remove the entirety of a cancer[1]. In fact, studies have shown that patient outcome is directly correlated to the surgeon's ability to completely remove the tumor. However, using today's surgical methods, it is oftentimes difficult to differentiate healthy tissues from cancerous tissues.

Computed tomography (CT) and position emission tomography (PET) have traditionally been the most commonly used imaging techniques used for the detection of cancers. CT scans use differences in electron density of tissues to differentiate healthy tissue from a lesion. In contrast, PET imaging detects areas where the uptake and metabolism of glucose is high. A radiopharmaceutical such as 2-[^{18}F] fluoro-2-deoxy-D-glucose (FDG) can be detected by a PET scan in a cancer because FDGs have a higher rate of metabolism in tumors than in most healthy tissue[2]. Unfortunately, however, CT scans and PET scans have limitations that restrict the sensitivity and specificity of their images. PET scans, for example, are problematic because other tissues such as the brain and liver display high glucose metabolism similar to tumors. Similarly, small molecules such as FDG are often seen during a PET scan in organs of the urinary system where they collect during excretion. As a result, it is difficult to differentiate cancerous tissue from background when there exists healthy tissues look identical to cancerous tissue on a PET scan[3]. To overcome the poor signal-to-

background ratio of CT and PET images, a group at The Ohio State University, headed by Dr. Edward Martin, has developed an alternative to CT and PET scans called radioimmunoguided surgery (RIGS) to increase the accuracy of surgical detection and removal of cancer[4].

RIGS is a cancer-detecting technique that utilizes a handheld probe for the detection of radioactive labeled (^{125}I-labeled) antibodies that bind specifically to cancerous tissue. The labeled antibody is injected into the patient prior to surgery and given sufficient time (sometimes several days) in the blood circulation to bind to its target, the cancer, and clear from the blood. Then, the handheld probe is used before, during, and after surgery to detect any cancerous tissue. This imaging tool is most valuable because it allows surgeons to intraoperatively determine the extent of local invasion of a tumor and the presence of remaining tumor after resection[5]. Any residual tumor that exists after initial resections can be identified and removed immediately at the time of the operation. The complete removal of a tumor in one operation eliminates the need for a second surgery and the concern that any residual tumor could proliferate. A comprehensive study by Martin, et al. of 212 patients with colorectal cancers (Figure 1) showed that patients who had the complete removal of all tissue identified by RIGS (Group A) lived significantly longer than those in whom tumor was unable to be removed (Group B and C)[2]. With an extremely sensitive probe that produces low background activity and immediate intraoperative information, RIGS is far superior to traditional imaging tools like CT and PET scans.

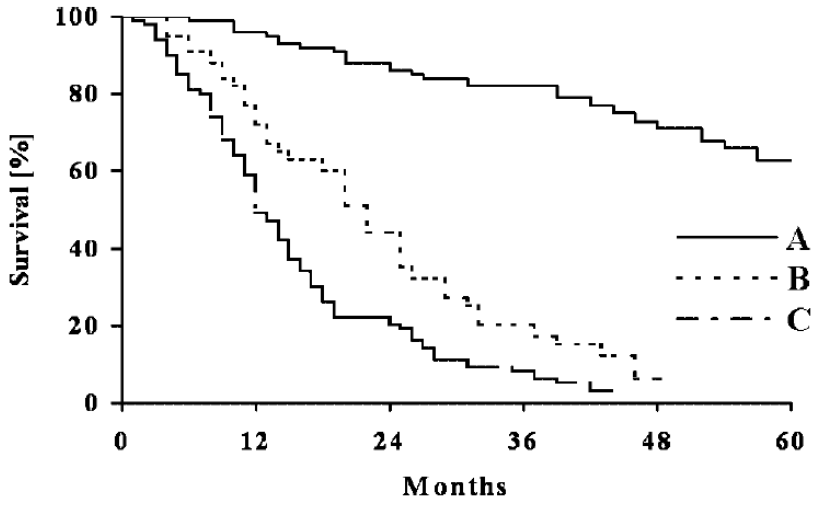

Figure 1. Survival benefit by RIGS with anti-TAG-72 antibodies[2]

1.2 Anti TAG-72 Antibodies of the Past and Present

A fundamental part of the RIGS systems is radioactive-labeled antibodies that bind specifically to cancer. The antibodies bind to a disaccharide called Sialyl-Tn, which is found in a glycoprotein called tumor-associated glycoprotein 72 (TAG-72)[6]. This glycoprotein is expressed at high levels in the mucin secreted by a variety of mucin-secreting cancers called adenocarcinomas, including colorectal, gastric, pancreatic, endometrial, breast, prostate, and ovarian, but is not found significantly on normal tissues[7-9]. Figure 2 illustrates the cell surface of an adenocarcinoma where Sialyl-Tn can be found in the mucin.

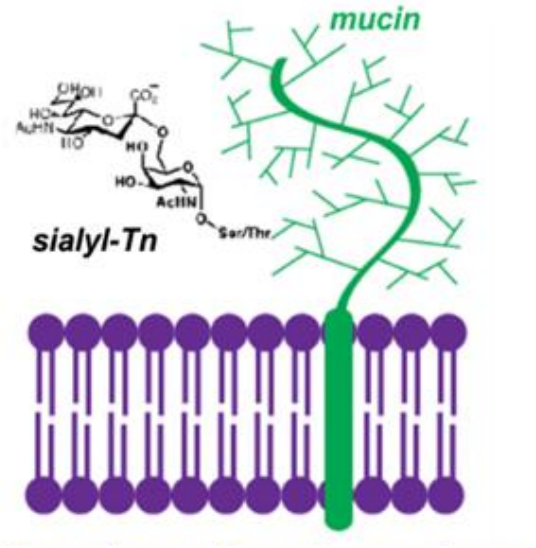

Figure 2. Cell membrane of an adenocarcinoma

Anti TAG-72 antibodies have proven the excellent potential of the RIGS system since it was first introduced in 1986. The first generation antibody designed for RIGS, B72.3, targeted a variety of adenocarcinomas but failed to bind to primary tumors or lymph nodes effectively[7,8]. Furthermore, when injected into patients with colorectal carcinoma, B72.3 elicited an undesirable pharmacokinetic property called the human anti-mouse immunoglobulin antibodies (HAMA) response, which results from the formation of immune complexes, either antigen-antibody or antibody-antibody complexes. Consequently, these complexes prevented effective targeting of the antibody to the antigen and detection of the antibody in patients[10-12]. To improve the binding limitations of B72.3, a second-generation antibody with higher affinity than B72.3 called CC49 was developed by the National Cancer Institute; however, it too elicited the HAMA response. As a result, a group in Korea headed by Sun Ok Yoon engineered a humanized form of CC49 called AKA by grafting only the

binding regions of CC49 onto a homologous human germ line. After observing a 2-fold lower affinity with AKA compared with CC49, Yoon et al. used random mutagenesis of one of the binding domains to engineer a number of variants, the highest affinity variant called 3E8 showing about 22 fold higher affinity than AKA. In 2005, 3E8 had the highest affinity and least number of mouse residues among all variants of B72.3 and CC49[13-16].

As shown in Figure 3, antibodies are large Y-shaped proteins consisting of two distinct regions: the constant region (the stem of the Y) and the variable region (the top of the Y). Each variable region consists of a heavy chain and a light chain and is responsible for binding to a specific antigen[17]. Due to their large size, full length antibodies like 3E8 have long serum half-lives and high normal tissue background. In an effort to engineer a smaller version of 3E8 with comparable affinity and stability as 3E8, the Magliery lab constructed a single chain variable fragment (scFv) called 3E8.scFv by connecting a heavy chain and a light chain of the variable region with a string of amino acids. This scFv has similar binding properties as full length 3E8; however, due to its reduced physical size (28 kilodaltons versus ~200 kilodaltons), 3E8.scFv clears the body much faster than 3E8, reducing its exposure to the tumor and thus limiting its use as a method to detect cancers intraoperatively. The Magliery lab has investigated the use of a variety of polyethylene glycol chains (PEGs) as a way to increase the size of 3E8.scFv and increase its serum half-life (plasma circulation time). Ideally, a PEGylated scFv, or a scFv that has been conjugated to one of multiple PEGS, will have an optimized serum half-life between that of the scFv and full length antibody (IgG), as illustrated in Figure 4.

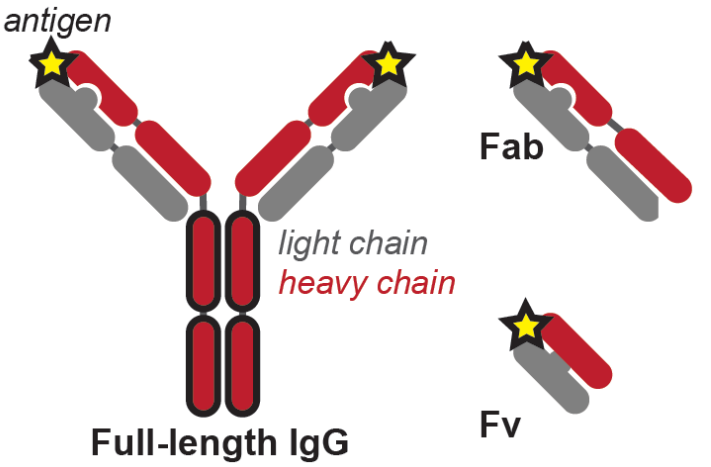

Figure 3. Structure of an antibody and scFv

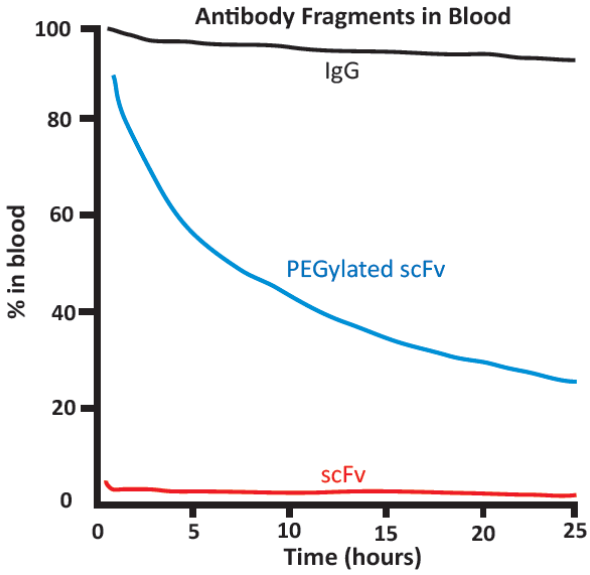

Figure 4. Optimized serum half-life

1.3 Modification of 3E8 Using Polyethylene Glycol Chains

1.3.1 Polyethylene Glycol (PEG)

Polyethylene glycol is a non-toxic, nonimmunogenic, hydrophilic, water soluble polymer that has been approved by the Food and Drug Administration (FDA) for its use in biopharmaceuticals. Commercial suppliers such as JenKem in China and Creative PEGWorks in the USA chemically synthesize PEGs of a variety of lengths up to 40 kDa and shapes, including linear and branched. In the past, PEGs have been synthesized using polymerization with broad polydispersity, meaning that they contained a large distribution of molecular masses; however, recently, stepwise, organic reactions have been used to narrow the molecular weight distribution and produce discrete PEGs with much lower heterogeneity[18,19]. To allow for conjugation to a wide variety of functional groups, PEGs are

terminated on either end during synthesis with hydroxyl groups and have the general structure shown in Figure 5[20].

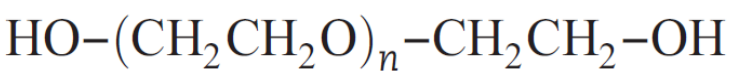

Figure 5. General structure of a PEG

1.3.2 Chemistry of PEGylation

PEGylation is the covalent attachment of polymer polyethylene glycol to a molecule, usually a protein or peptide. As discussed earlier, PEGs are able to react with a variety of functional groups, most commonly the amine and thiol groups of amino acids in a protein. Lysine, which contains an amine group, is one of the most prevalent amino acids found in proteins and is often found on the surface of proteins, making it easily accessible for PEG reactions. Since a single protein usually contains more than one lysine, a heterogeneous mixture of conjugated molecules is often produced, each molecule differing in the number and site of the conjugated PEG chains. For this reason, PEGylation at lysines in often termed non-specific or random PEGylation. In order for a PEG to react at a particular function group, it is first activated by reacting a particular organic molecule with the hydroxyl group of the PEG. Figure 6 illustrates the chemical reaction between a *N*-hydroxysuccinimide-ester (NHS-ester) activated PEG and an amine group[20].

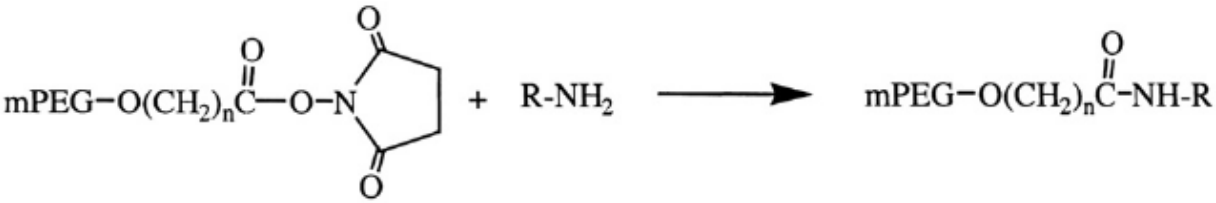

Figure 6. Chemical reaction of NHS-ester activated PEG and amine group

Another commonly PEGylated but less prevalent residue on the surface of proteins is free cysteine, which contains a thiol functional group. When a protein does not contain any unpaired cysteines for PEGylation, one or more can be genetically engineering into the protein to allow for what is called site-specific PEGylation. Recently, there has been a trend away from non-specific PEGylation and towards site-specific PEGylation because the latter produces a homogenous product containing only singly conjugated material. PEGs to be reacted with free cysteines are first activated by maleimide chemistry. The activated PEG is then reacted with the thiol group to produce a conjugated cysteine, as shown in Figure 7[19,20].

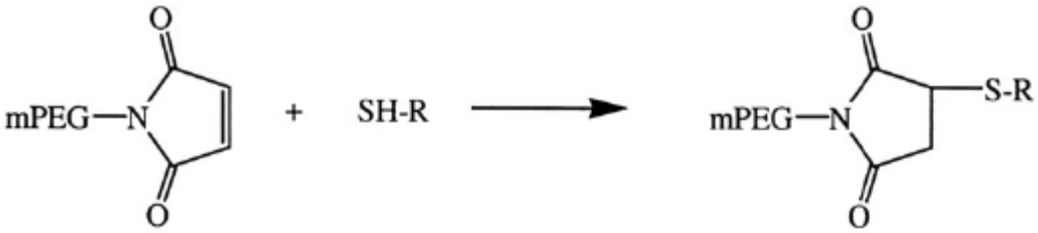

Figure 7. Chemical reaction between maleimide-activated PEG and thiol group

1.3.3 Theranostic Uses for PEGylation

Since the approval of PEGs in 1990, PEGylation has been widely used to improve a number of suboptimal physiochemical and pharmacokinetic properties such as limited solubility, proteolytic instability, short serum half-life, and immunogenicity of peptides and proteins. In fact, the PEGylation of proteins has been so successful that as many as nine different PEGylated products have been approved by the FDA for the treatment of such conditions as severe combined immunodeficiency disease (SCID), ocular vascular disease, hepatitis C, Crohn's disease, and rheumatoid arthritis[19,22].

Figure 8 provides an illustration of some of the ways in which PEGylation directly improves proteins. As described earlier in the discussion of anti-TAG-72 antibodies, antibodies have the potential to elicit immunogenic reactions when injected into patients. This concern has prompted the use of PEGylation to reduce their toxicity and improve their safety during administration. The PEG chains, when conjugated to a protein like an antibody, can shield the surface of the antibody from the environment where proteolytic enzymes may exist, thereby increasing the stability of the molecule[19,21]. Additionally, PEGs can improve circulating half-lives of conjugated antibodies by increasing the apparent size of the molecule to above the size filtered by the kidneys. During circulation, blood passes through a structure of the kidneys called the glomerulus, which removes anything below 30 kDa for urinary excretion. Anything greater than this size will remain in the blood for a time that can be tuned using PEGs of different shapes and lengths[21]. Furthermore, PEGs can increase the solubility of a protein in many solvents due to the presence of both hydrophobic and hydrophilic groups on the PEG. Consequently, PEGylated proteins can achieve higher concentrations in solution without causing aggregation, which can be important when considering dosing options for patients[23]. With the rapidly growing interest in research and development of antibodies as therapeutics, the use of PEGs to enhance the properties of these molecules is becoming an equally exciting area of research.

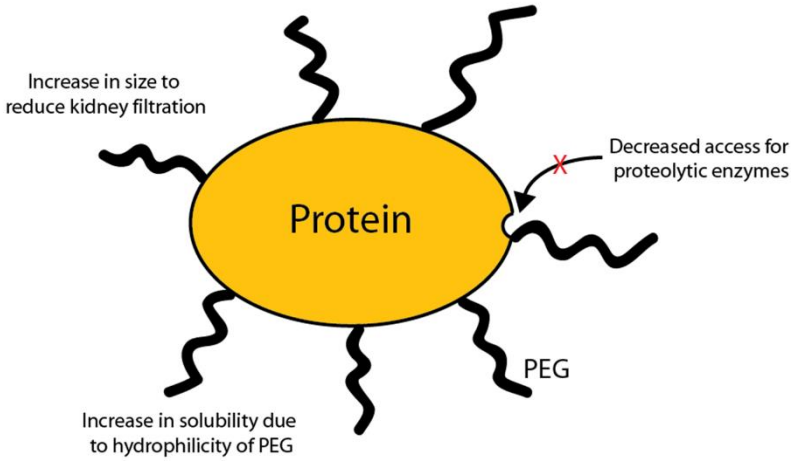

Figure 8. Advantages of PEGylated protein

1.4 Characterization of PEGylated Proteins

While it is known how PEGs in general can influence the characteristics of a protein, a variety of tools and techniques can be used to study the effects that PEGs of various shapes and lengths can have on a particular protein's biophysical characteristics. In the case of an antibody, the study of its thermal stability, affinity to the antigen, size, and shape post PEGylation is extremely valuable for its potential as a therapeutic. To measure the temperature at which the antibody unfolds, differential scanning fluorimetry (DSF) can be used. This technique utilizes a fluorescent dye that binds to the hydrophobic parts of the protein, which are most often found within the core of the protein. As the temperature of the antibody and dye mixture slowly increases, the antibody unfolds and the dye-associated hydrophobic residues are gradually exposed[24]. Meanwhile, the instrument measures the increase in fluorescence, eventually producing the graph shown in Figure 9, which can be fitted to determine the melting temperature of the protein[24].

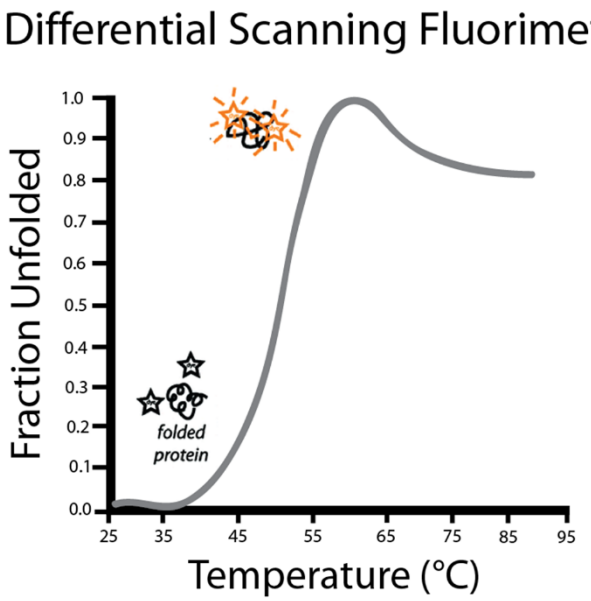

Figure 9. Typical unfolding pattern seen in DSF

Just as important as an antibody's stability after PEGylation is its ability to retain binding to its antigen. Surface plasmon resonance (SPR) is an optical-based assay that measures the kinetics of interactions between two molecules such as an antibody and an antigen. First, a gold chip coated in carboxymethylated dextran is immobilized with the antigen using a particular type of chemistry dependent on the ligand. Then, the solution of antibody is flowed over the chip at a constant rate. Meanwhile, as illustrated in Figure 10, a beam of light is projected onto the opposite surface of the chip, and the angle of refraction of this light is measured in real time. If binding to the antigen occurs, the refractive index changes, causing a change in the angle of refraction. After the antigen reaches saturation, the antibody is gradually dissociated from the antigen by flowing buffer over the plate, during which the angle of refraction again changes and is measured[25]. The resulting data is then fit using a computer program that calculates association and dissociation rate constants, with the ratio of the two yielding the affinity constant[26].

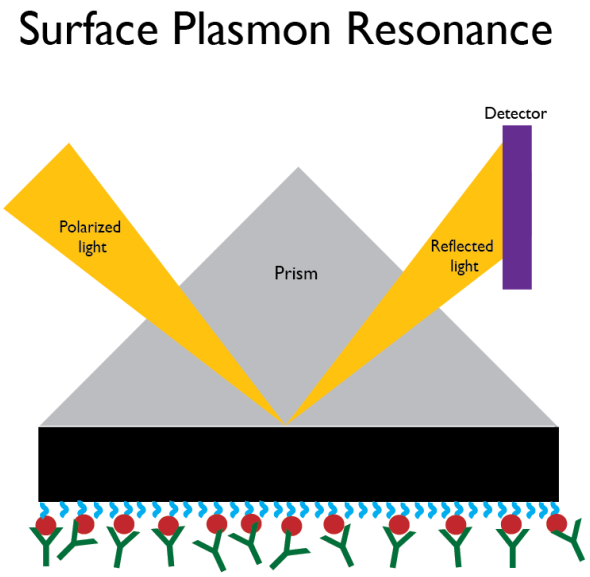

Figure 10. Setup of SPR experiment

A variety of tools can be used to determine the shape and size of a PEGylated protein. Gel filtration chromatography is a purification technique that uses a porous column to separate molecules based on their size. The molecules pass through the column at rates that are directly proportional to their size: proteins of smaller molecular weight come off the column slower than larger molecules because smaller molecules travel through the beads, making their path through the column longer than the larger molecules[27]. In addition to its use for purification, gel filtration can be used to study the sizes of molecules with respect to each other, for example the sizes of a protein conjugated to various lengths and shapes of PEGs. Also, gel filtration can indicate any aggregation of protein after PEGylation, through the formation of dimers, trimers, and higher oligomeric states.

For a more definitive measurement of size, a technique called analytical ultracentrifugation (AUC) can be used to determine the shape and size of molecules in solution by centrifuging the sample at high speed and analyzing sedimentation with hydrodynamic theory. A detector takes absorbance measurements at known times in order to

determine the concentration distribution of the sample. Figure 11[28] provides an illustration of the setup of a typical AUC experiment. During AUC, samples are characterized in their native state, under nondestructive conditions such that they can be recovered for further characterization[29].

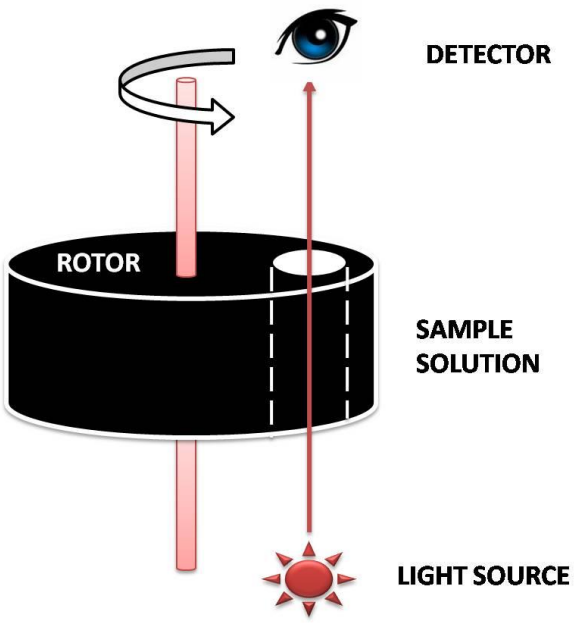

Figure 11. Setup of AUC experiment[28]

1.5 Preliminary Studies of PEGylated 3E8.scFv

As mentioned at the end of section 1.2, the Magliery lab in interested in conjugating 3E8.scFv to various types of PEGs in order study the effects of PEGylation on various biophysical and pharmacokinetic characteristics. First, 3E8.scFv was PEGylated non-specifically (at lysines) with a set of discrete NHS-ester PEGs varying in size and shape. For each type of PEG, the reaction with 3E8.scFv was done with low loads of PEG (an average

of about one or two attached PEGs per molecule) and medium loads of PEG (an average of about five attached PEGs per molecule). Then, each PEGylated sample was characterized using many of the techniques discussed in the previous section including DSF and SPR. Figures 12 and 13 show the DSF results for the non-specific PEGylation of 3E8.scFv at low and medium loads, respectively. The thicker black line represents unPEGylated 3E8.scFv, while the colored lines are of PEGylated samples. Taken together, this data showed that low loads of non-specific PEGylation did not seem to affect thermal stability; however, higher loads of PEGylation seemed to decrease the melting temperature of the sample.

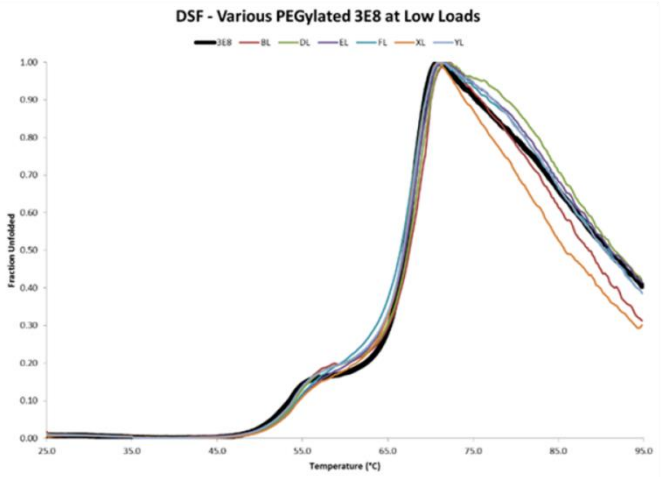

Figure 12. Melting curves of 3E8.scFv PEGylated at low loads

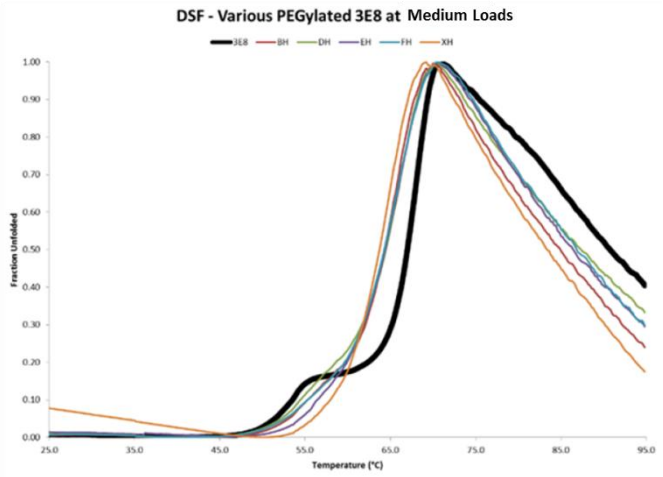

Figure 13. Melting curves of 3E8.scFv PEGylated at medium loads

In fact, a similar trend was seen after studying the binding of PEGylated 3E8.scFv to TAG-72 using SPR. Figure 14 provides a comparison of the data between low and medium loads of PEGylation. At low loads, the dissociation constant (K_D) remains relatively close to that of unPEGylated 3E8.scFv. However, medium loads of PEGylation dramatically ablated binding, supporting the conclusion that medium of loads of PEGylation at surface lysines

decreases the stability and affinity of 3E8.scFv[30]. It seems possible that there may be specific lysines in the protein that when PEGylated greatly affect stability and binding. A focus of this thesis is to pinpoint lysines, perhaps near the binding site of the antibody fragment that may be responsible for the shift in character seen at higher loads of modification.

Sample	K_D	
3E8.scFv	12 nM	
PEG	**Low**	Medium
B	13 nM	>1 µM
D	31 nM	>1 µM
E	30 nM	230 nM
F	26 nM	41 nM
X	15 nM	>1 µM
Y	20 nM	-

Figure 14. Dissociation constants for 3E8.scFv PEGylated at low and medium loads

To understand the effects of modifying a single residue within 3E8.scFv, a new version of 3E8.scFv called 3E8.scFv.Cys was engineered to contain a free cysteine residue at the C-terminus of the antibody fragment. This cysteine residue was specifically modified with four unique PEGs of different sizes and shape using maleimide chemistry. Similar to the characterization of PEGylated 3E8.scFv, the thermal stability and binding of PEGylated 3E8.scFv.Cys was determined. The DSF data, shown in Figure 15, was difficult to understand because a large unfolding curve was much more pronounced in the PEGylated samples than in the unPEGylated control (3E8.scFv.Cys). Nonetheless, it appeared that PEGylation at cysteine, regardless of the size of the PEG, affected the unfolding pattern of the conjugated protein significantly. In terms of the binding of these PEGylated samples to

TAG-72, the dissociation constants were unchanged between unPEGylated and PEGylated 3E8.scFv.Cys, each showing slightly weaker binding than 3E8.scFv. In addition to stability and affinity, aggregation of the PEGylated samples was studied through gel filtration. This data showed that each of the samples still existed solely as monomers and no higher order oligomeric states were present. PEGylated 3E8.scFv.Cys has a high potential as a cancer therapeutic because of its strong affinity to TAG-72 and its certainty with regards to the site of PEGylation[30]. However, further characterization needs to be completed to understand additional structural questions such as the way that the PEG interacts with the protein.

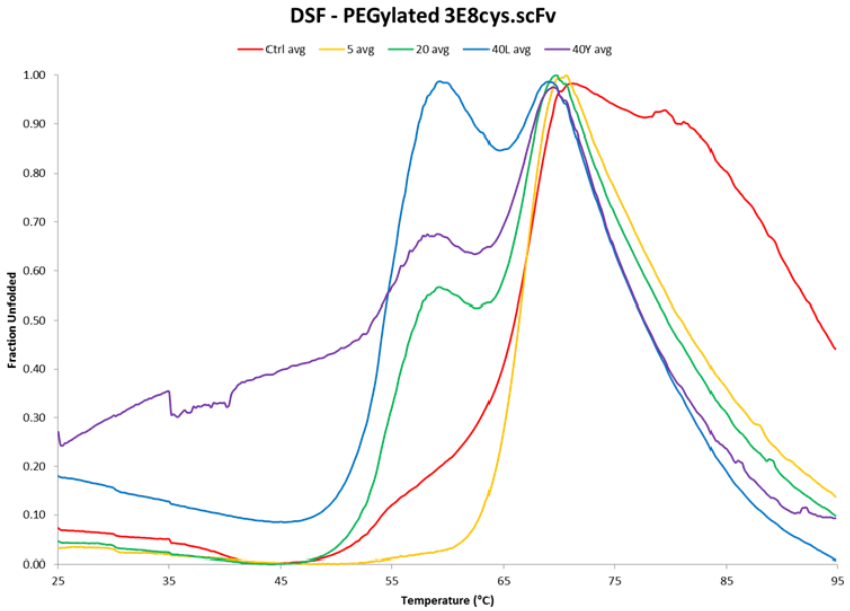

Figure 15. Melting curves of PEGylated 3E8.scFv.cys

1.6 3E8.scFv for Immunohistochemical Analysis

Immunohistochemistry (IHC) is a tool used in pathology laboratories for the visualization, diagnosis, and characterization of cancers. More specifically, it can be used to distinguish between various types of cancers, help determine the stage of a cancer, and identify post-surgical margins (positive, negative, and close)[31]. Currently, a variety of

antibodies, many of which are commonly used together, exist to target certain epitopes on cancers. For the diagnosis of adenocarcinomas, antibodies such as B72.3 and CC49 (mentioned earlier in section 1.2) are used in commercially available kits[32]. While B72.3 and CC49 have shown proof of principle, the Magliery lab would like to use a variant of 3E8.scFv called 3E8.scFv.FLAG as an alternative for the diagnosis and analysis of cancers like adenocarcinomas. 3E8.scFv.FLAG utilizes a C-terminal FLAG tag (sequence: DYKDDDDK) for enhanced immunohistochemical staining and is known to bind better to TAG-72 than the first and second generation antibodies. Figure 16 (designed by Dr. Brandon Sullivan) offers an illustration of the IHC scheme involving 3E8.scFv.FLAG that the Magliery lab is currently investigating. First, the primary antibody (3E8.scFv.FLAG) is bound to the antigen (in this case a sugar called Sialyl-Tn). Then, the secondary antibody (anti-FLAG Biotin conjugate), which is conjugated to multiple biotin molecules, is bound to the primary antibody. The tertiary agent (streptavidin HRP conjugate) binds to the secondary antibody via the strevtavidin-biotin linkage, the strongest known non-covalent interaction between a protein and a ligand. The HRP (horseradish peroxidase) enzyme picture in yellow then reacts with its substrate, 3,3'-diaminobenzidine (DAB) to produce a brown precipitate that is easily visualized. Figure 17 shows a section of an adenocarcinoma stained by Kristin Miller at the OSU Wexner Medical Center with a biotinylated version of 3E8.scFv that was engineered by Dr. Brandon Sullivan. An image like this could be further analyzed by a pathologist to identify specific locations of staining within each cell.

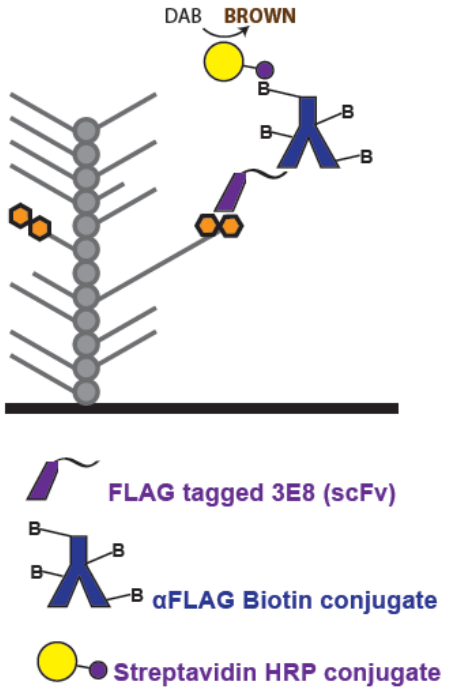

Figure 16. IHC scheme of 3E8.scFv.FLAG with anti-FLAG Biotin conjugate

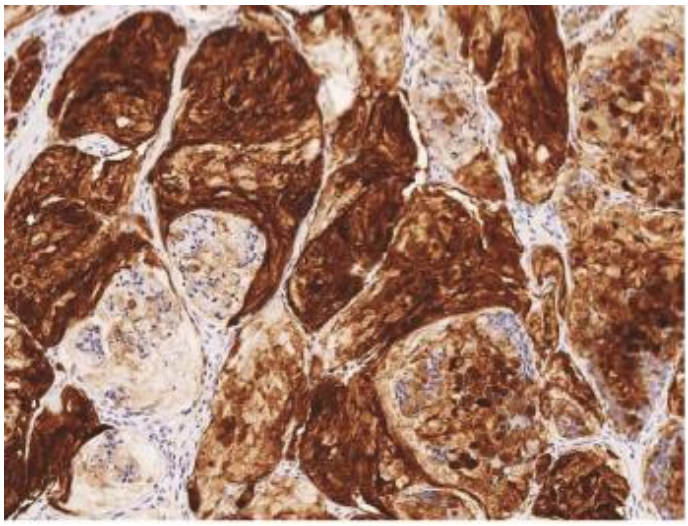

Figure 17. Adenocarcinoma stained with anti-TAG-72 antibody

Chapter 2: Objectives

2.1 Identification of and Mutations to PEGylated Lysines

Numerous tools will be used in order to locate potentially problematic lysine residues that may be responsible for the shift in character of 3E8.scFv at medium amounts of modification. Once located, these residues will be systematically replaced with arginine, a residue similar in size and structure but that cannot be modified by PEGylation. By eliminating possible locations for modification, the goal is to determine which sites are problematic, while simultaneously engineering a stable form of 3E8.scFv that can be modified at high loads without a dramatic change in biophysical properties.

2.2 Expression and Purification of 3E8.scFv Constructs

The proteins of interest must be produced in enough quantities in order to investigate their properties and potential as a tool for Radioimmunoguided surgery. Various versions of 3E8.scFv will be expressed and purified, including 3E8.scFv (for use in NHS-ester PEGylation), 3E8.scFv.Cys (for use in maleimide PEGylation), and 3E8.scFv.FLAG (for use in immunohistochemistry).

2.3 Non-specific PEGylation at Lysines and Characterization

After engineering new forms of 3E8.scFv with mutations to specific residues, these proteins will be modified by NHS-ester PEGylation. A variety of biophysical techniques can be used to study the thermal and kinetic effects of modifying numerous lysines in the molecule. The results of these experiments will determine whether the problematic residues

were successfully located and if a stable version of 3E8.scFv for non-specific PEGylation was engineered.

2.4 Specific PEGylation at Cysteines and Characterization

To study the effects of PEGylation at a single site, 3E8.scFv.Cys will be PEGylated using maleimide chemistry. PEGylated 3E8.scFv.Cys can be analyzed using the same tools used for NHS-ester PEGylated samples. In addition, its shape and size after PEGylation will be studied to potentially understand the PEG's characteristics once attached to the protein. It is possible that PEGs of various sizes and shapes will interact differently with the protein after conjugation.

2.5 Optimization of 3E8.scFv.FLAG for Immunohistochemistry

3E8.scFv.FLAG is a mutant of 3E8.scFv that differs only by the addition of a C-terminal FLAG tag, which is important for immunohistochemistry. The concentrations of antigen, primary and secondary antibodies, and development agents will be optimized in order to produce a sensitive and reliable in vitro detection method for adenocarcinomas.

Chapter 3: Materials and Methods

3.1 Identification of and Mutations to PEGylated Lysines

3.1.1 PyMOL

PyMOL is a molecular graphics software that can be used to produce 3-D images of small biological molecules, such as proteins (Schrödinger, Inc.). Using the X-ray crystal structure of homologous proteins to 3E8, the program generated a rendering of the protein's predicted structure, depicting possible interactions between domains. Of most interest for this project was the location of particular lysines residues with respect to the binding domain of the protein.

3.1.2 Mass Spectrometry

Mass Spectrometry was performed on NHS-ester PEGylated (method described in section 3.3.1) 3E8.scFv by Mengxuan Jia in the Wysocki Lab at The Ohio State University. The samples were first digested with trypsin in solution at 37 °C for 3 hours. A second digestion was performed in gel for one hour at 50 °C. Then, the samples were cleaned using C18 solid phase extraction and analyzed by liquid-chromatography mass spectrometry (LCMS) using a Velos Pro Dual-Pressure Linear Ion Trap Mass Spectrometer. The location and frequency of PEGylated lysines in 3E8.scFv was analyzed by the Proteome Discoverer 1.4 software.

3.1.3 Site-Directed Mutagenesis

Oligonucleotides containing lysine to arginine point mutations at the 24, 36, 109, 146/147, 157, 193, 197, and 208 positions of 3E8.scFv were purchased from Sigma-Aldrich. With the help of David Alten, a previous undergraduate, the thermodynamic properties of these oligonucleotides were optimized using OligoTech. The genes were constructed using site-directed mutagenesis PCR, in which the sense and antisense primers anneal to the template strand of DNA in two separate reactions, producing two mutagenic fragments. After these fragments were annealed together, the reassembled gene was amplified using amplification primers that create endonuclease sites within the gene for digestion and ligation. Table 1 lists the sequences of the oligonucleotides used to engineer these mutants. Each mutagenic primer is bolded where the point mutation was inserted. Amplification primers 1 and 2 were used for each variant and designed by graduate student Nick Long.

Primer	Sequence (5'-3')
K24R	GGCGAACGTGCGACGATTAATTGC**AGG**AGTAGCCAGAGCGTG CTTTACAGC GCTGTAAAGCACGCTCTGGCTACT**CCT**GCAATTAATCGTCGCA CGTTCGCC
K36R	AGCGTGCTTTACAGTAGTAACAAT**AGG**AATTACCTGGCGTGGT ATCAGCAA TTGCTGATACCACGCCAGGTAATT**CCT**ATTGTTACTACTGTAAA GCACGCT
K109R	CCATTGACATTCGGGGGAGGCACC**AGA**GTGGAGATCAAACTGA GCGCGG CCGCGCTCAGTTTGATCTCCAC**TCT**GGTGCCTCCCCCGAATGTC AATGG
K146R, K147R	CTGGTACAGTCGGGTGCGGAAGTG**AGGAGA**CCTGGGGCGTCG GTGAAAGTGAGC GCTCACTTTCACCGACGCCCCAGG**TCTCCT**CACTTCCGCACCC GACTGTACCAG
K157R	GGCGTCGGTGAAAGTGAGCTGC**AGA**GCGAGTGGCTATACCTTT ACCG CGGTAAAGGTATAGCCACTCGC**TCT**GCAGCTCACTTTCACCGA CGCC
K193R	CCCCAGGCAACGATGATTTC**AGG**TATTCACAGAAGTTCCAAGG GC GCCCTTGGAACTTCTGTGAATA**CCT**GAAATCATCGTTGCCTGG

	GG
K197R	AACGATGATTTCAAGTATTCACAG**AGG**TTCCAAGGGCGCGTGACCATTACC GGTAATGGTCACGCGCCCTTGGAA**CCT**CTGTGAATACTTGAAATCATCGTT
K208R	CGCGTGACCATTACAGCCGAT**AGA**AGTGCAAGCACCGCGTATATGG CCATATACGCGGTGCTTGCACT**TCT**ATCGGCTGTAATGGTCACGCG
Amplification 1	ATTATTATTCATATGAAATATCTGTTACCTACTGCTGC
Amplification 2	AATAATGGATCCTTAGCTGCTCACGGTCAC

Table 1. Oligonucleotides used to engineer 3E8.scFv lysine to arginine constructs

Each amplified gene and pHLIC vector were digested with BamHI and NdeI (NEB). The digested gene was ligated into the digested vector using T4 DNA Ligase (NEB) in an overnight reaction at 16 °C. The ligation was transformed into DH10B Competent cells, recovered with 1 mL of 2YT media, and plated onto an antibiotic plate which was incubated overnight at 37 °C. The following day, multiple colonies were picked for overnight growth in 5 mL of 2YT media with 0.1 g/L antibiotic. The DNA was purified from the cells using the Qiagen Miniprep protocol and sequenced at either Genewiz (New Jersey) or Genomics Shared Resource (The Ohio State University).

3.2 Expression and Purification of 3E8.scFv Constructs

Each of the 3E8.scFv constructs described here (3E8.scFv, 3E8.scFv.Cys, and 3E8.scFv.FLAG) was expressed and purified using the same conditions. For expression, 1 µL of miniprep containing the gene of interest inserted into pHLIC vector was transformed into C43(DE3) *E. coli* cells and immediately recovered with 1 mL of media. After incubation at 37 °C for 30 minutes, 150 µL were plated on an antibiotic plate using a tertiary streak and

incubated overnight at 37 °C. The next day, a seed culture was grown by inoculating 1 colony from the previous night's plate into 25 mL of 2YT media containing 1 mM antibiotic and 1 mL of 20% glucose. This seed culture was grown overnight at 37 °C and inoculated into 1.5 L of 2YT media containing 0.1 g/L antibiotic in a 4L non-baffled flask. The 1.5 L culture was grown in a shaker at 37 °C and shaken at 200 rpm until OD_{600} was in the range of 0.5-1.0. Then, the culture was cold-shocked by moving it to 4 °C for 30 minutes before induction with 0.05 mM IPTG. After incubating the culture for 30 minutes more at 4 °C, it was grown overnight at 16 °C in the shaker at 120 rpm.

The following day, the culture was centrifuged for 10 minutes at 5,000 rpm and 4 °C in 1 L centrifuge tubes. The resulting pellet was resuspended in 25 mL of protein L binding buffer (56.1 mM Na_2HPO_4, 144.2 mM NaH_2PO_4, 150 mM NaCl, pH 7) per liter of culture and 5 mM $MgCl_2$, 0.5 mM $CaCl_2$, 5 µL of DNase I and RNase A, 30 mg of lysozyme and 0.1% Triton X-100. The mixture was allowed to stir on ice for 30 minutes. Then, the cells were lysed at 4 °C using the EmulsiFlex (Avestin), which utilizes 3 cycles of high pressure (between 15,000 and 20,000 psi) to homogenize the cells. Following lysis, the cell lysate was centrifuged for 45 minutes at 15,000 rpm in SS34 tubes. After the first round of centrifugation, the supernatant was again centrifuged for 45 minutes at 15,000 rpm. The resulting supernatant was collected for affinity chromatography purification using a HiTrap Protein L column (GE Healthcare Life Sciences).

1 mL or 5 mL HiTrap Protein L columns were used for purification depending on the size of the cell culture. For each of the steps, a flow rate of 1.0 mL/min (1 mL column) or 5.0 mL/min (5 mL column) was used. First, the column was washed with 1 column volume (CV) of distilled water to remove the storage solution (20% ethanol). Then, the column was

equilibrated with 5 CV of protein L binding buffer, and the supernatant was loaded onto the column. The column was washed with 10 CV of protein L binding buffer, and the protein was eluted with 2 fractions (1 mL column) or 6 fractions (5 mL column) of 5 mL protein L elution buffer (100 mM glycine, pH 3). The column was cleaned with 5 CV protein L binding buffer, 5 CV 18 MΩ-cm H_2O, 5 CV regeneration buffer (6 M Guanidine HCl, 200 mM HOAC), 5 CV 18 MΩ-cm H_2O, and 5 CV 20% ethanol (storage solution).

The elution fractions containing the protein of interest were pooled together and the resulting sample was dialyzed into lysis buffer (50 mM Tris-HCl, 300 mM NaCl, 10 mM imidazole, pH 8) with 1 mM TCEP for 3E8.scFv.Cys only. 200 µL of in-house TEV protease and 1 mM DTT were added to the sample and allowed to incubate overnight at room temperature. The next morning, 100 µL of additional TEV protease and 1 mM DTT were added to the sample for incubation until the afternoon, at which point the sample was dialyzed into ion exchange buffer A (50 mM potassium acetate, 15 mM NaCl, pH 5) for cation exchange chromatography using a 1 mL RESOURCE S column (GE Healthcare Life Sciences).

The 1 mL RESOURCE S column was connected to the ÄKTApurifier FPLC (GE Healthcare Life Sciences), washed with 10 CV of 18 MΩ-cm H_2O, and equilibrated with 20 CV of ion exchange buffer A. The sa*m*ple was loaded onto the column using a Superloop, washed with 2 CV of ion exchange buffer A, and eluted from the column using a 200 CV gradient (from 15 mM NaCl to 1 M NaCl) with ion exchange buffer B (50 mM potassium acetate, 1 M NaCl, pH 5). During the run, the flow rate was increased so much that the pressure limit (1.5 MPa) was not exceeded. Furthermore, during the elution phase, the gradient was temporarily held when the UV signal quickly rose, indicating the elution of a

species from the column. Once the gradient reached 1 M NaCl, the fractions were analyzed using gel electrophoresis and any fraction containing the protein of interest were pooled together for dialysis into PBS (137 mM NaCl, 2.7 mM KCl, 10 mM Na_2HPO_4, 2 mM KH_2PO_4, 1 mM TCEP for 3E8.scFv.Cys only) for storage at 4 °C.

3.3 Non-Specific PEGylation at Lysines and Characterization

3.3.1 NHS-ester PEGylation

A protocol by Thermo Scientific was followed for NHS-ester PEGylation of lysines. First, the 1.8 kD PEG (Quanta BioDesign) was removed from storage at -20 °C and allowed to equilibrate to room temperature before opening. A stock solution of PEG was made by dissolving a certain amount of PEG in dimethylformamide (DMF) or dimethyl sulfoxide (DMSO). Based upon the desired excess of PEG to protein, the appropriate volume of this PEG solution was mixed with 450 µL of the protein, which was stored in PBS, an amine-free buffer to prevent NHS-Tris reactions. Calculations were performed to ensure that the total amount of organic material (the PEG solution) was kept under 5% to prevent damage to the protein's folding. The reaction was brought up to 500 µL with PBS and incubated at room temperature for one hour. To quench the reaction, 100x excess of ethanolamine to the amount of PEG was added to the reaction. The extent of PEGylation was determined by SDS-PAGE.

3.3.2 Differential Scanning Fluorimetry (DSF)

The stock solution of 5000x SYPRO Orange dye (Thermo Scientific) was diluted to 300x in PBS. To achieve a final concentration of 15x, 1 µL of 300x dye was mixed with 19 µL of protein (in PBS) in a 96-well 0.2 mL thin-wall PCR plate (USA scientific). The plate was sealed with Adhesive PCR Film (Thermo Scientific) after all samples were prepared. All

of this was done in the darkest setting to avoid activation of the light-sensitive dye. The experiment was performed using a program on a BioRad C1000 Thermal Cycler that increases the temperature of the protein solution by 0.2 °C every 12 seconds from 25 °C to 95 °C and measures the fluorescence at each point. The resulting melting curves were normalized and analyzed in Microsoft Excel.

3.3.3 Surface Plasmon Resonance (SPR)

Surface Plasmon Resonance was performed in the Plant-Microbe Genomics Facility at OSU using a Biacore T100. A CM5 sensor chip (GE Healthcare Life Sciences) was immobilized with 0.5 mg/mL BSM (the antigen) and 0.016 mg/mL BSA (the negative control) using immobilization buffer (100 mM NaAc, pH 4) and an Amine Coupling kit (1-ethyl-3-(3-dimethylaminopropyl)carbodiimide hydrochloride (EDC), N-hydroxysuccinimide (NHS), and ethanolamine hydrochloride-NaOH (pH 8.5)). Previous scouting by postdoctoral researcher Brandon Sullivan determined that these conditions were most ideal. After washing the chip with 50 mM NaOH until a target level of 700 response units was reached, the samples were analyzed in HBS buffer (10 mM HEPES, 150 mM NaCl, 3.4 µM EDTA, 0.005% Tween-20, pH 7.4). In order to accurately study the protein's affinity to the antigen, the program suggests preparing a range of concentrations of protein which can be analyzed and then fit to a curve. Concentrations of 0, 5, 10, 25, 50, 75, 75, 100, 150, and 200 nM were used for each protein. Each of these concentrations was flowed over the chip for 120 seconds at a flow rate of 10 µL/minute and dissociation time of 180 seconds. Then, the chip was regenerated by flowing regeneration buffer (6 M GuHCl, 200 mM HOAc) over the chip for 30 seconds at a flow rate of 30 µL/minute and a stabilization period of 0 seconds. Following

the completion of all 10 concentrations, the data was fit over all concentrations in the Biacore Evaluation software using a 1:1 global fit and a local fit for R_{max}, to output a k_a, k_d, and K_D.

3.4 Specific PEGylation at Cysteines and Characterization

3.4.1 Maleimide PEGylation

The procedure used for maleimide PEGylation is similar to that of NHS-ester PEGylation. The PEG was removed from -20 °C and allowed to equilibrate to room-temperature before a stock solution containing a calculated amount of PEG was made in PBS. Then, a certain volume of this stock solution was added to the protein solution in PBS to achieve the desired excess of PEG to protein. Different from the NHS-ester protocol, the PEG solution was added to the protein solution in increments because the PEGs used for maleimide PEGylation were much larger and more concentrated than those used for NHS-ester PEGylation. After combining the two solutions, the reaction was incubated at room temperature overnight and quenched the following day by moving it to 4 °C. 5, 20, and 40 kD PEGs used for this experiment were purchased from JenKem Technologies, USA.

3.4.2 Gel Filtration

A 25 mL Superdex 75 10/300 GL size exclusion chromatography column (GE Healthcare Life Sciences) was connected to the same ÄKTApurifier FPLC described in section 3.2. The column was washed with 2 CV of 18 MΩ-cm H_2O and equilibrated with 2 CV gel filtration buffer (50 mM Tris, 100 mM NaCl, pH 8.0). The sample, which was earlier dialyzed into gel filtration buffer, was loaded onto the column using a 200 µL loop. Next, the column was washed with 25 mL gel filtration buffer using a constant flow rate.

3.4.3 Differential Scanning Fluorimetry (DSF)

The same protocol discussed in section 3.3.2 was used.

3.4.4. Surface Plasmon Resonance (SPR)

The same protocol discussed in section 3.3.3 was used.

3.4.5 Analytical Ultra Centrifugation (AUC)

Analytical Ultra Centrifugation was performed at The Ohio State University using a ProteomeLab XL-A (Beckman Coulter). 500 µL of PEGylated sample in PBS was loaded into a cell that sandwiches the sample between two quartz windows.

3.5 Optimization of 3E8.scFv.FLAG for Immunohistochemistry

3.5.1 Western Blots

The protein(s) to be studied were loaded and run on a 12.5% SDS-PAGE gel with rainbow marker (GE Amersham). The gel was transferred to nitrocellulose paper (HyBond ECL from GE Amersham) at 200 V for 1 hour, 20 minutes in transfer buffer (25 mM Tris base, 192 mM glycine, 10% methanol). The membrane was washed three times with PBST (PBS with 0.05% Tween-20) with 5 minute incubations on an orbital mixer between washes. To block the membrane, it was incubated overnight with 5% bovine serum albumin (BSA) at 4 °C. The next day, the BSA was washed off with 3 washes of PBST and the primary antibody was incubated with the membrane overnight at 4 °C. After 5 washes with PBST, the membrane was either developed with a 1:1 mixture of hydrogen peroxide (0.02%) and 1 mg/mL diaminobenzidine (DAB) in 50 mM Tris buffer (pH 7.2) or incubated with a secondary agent for one hour at room temperature, depending on the experiment. Following

the application of the secondary agent (if applicable), it was washed off five times with PBST and developed with H_2O_2/DAB. All dilutions were done in PBS buffer.

3.5.2 Dot Blot

The antigen (bovine submaxillary mucin, Sigma Aldrich) was spotted using a pipet tip onto the pencil marked corner of a nitrocellulose square. The membrane was incubated at room temperature for one hour before being blocked with 10 mg/mL BSA overnight. The next day, the BSA was washed off 3 times with PBST, with 5 minute incubations between washes on an orbital mixer. The primary antibody was incubated with the membrane for 1.5 hours and then washed off 3 times with PBST. Next, the secondary antibody was incubated with the membrane at room temperature for 1 hour. After 5 washes with PBST, the membrane was either developed with H_2O_2/DAB or incubated with the tertiary agent for 2 hours at room temperature, similar to the procedure for western blots. If a tertiary agent was used, it was washed off five times before development. All dilutions were performed in PBS buffer.

Chapter 4: Results and Discussion

4.1 Identification and Mutations to PEGylated Lysines

4.1.1 PyMOL and Mass Spectrometry

Figure 18 shows a 3-D molecular prediction of the structure of 3E8.scFv. The residues represented by spheres are surface-exposed lysines that have the potential to react with NHS-ester activated PEGs. During our initial examination of this structure, we located five lysines (24, 36, 157, 193, 208) that were located either within or near the binding sites, indicated by purple in figure 18. We hypothesized that these residues could be responsible for the loss of binding of the protein after higher loads of PEGylation if the PEGs were to interact with the binding sites and block the interface from binding to the antigen.

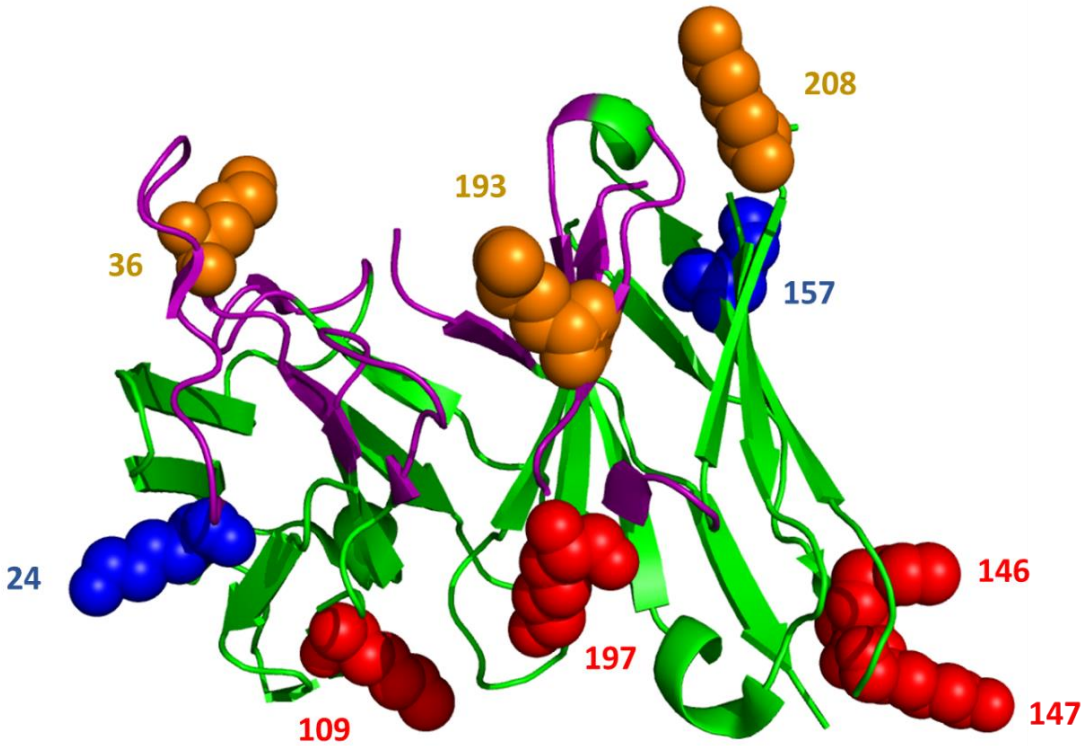

Figure 18. PyMOL rendering of 3E8.scFv with lysines highlighted

To further understand the frequency and location of NHS-ester PEGylation within 3E8.scFv, NHS-ester PEGylated 3E8.scFv was sent to the Wysocki Lab at The Ohio State University for analysis by liquid-chromatography mass spectrometry (LCMS). Figure 19 shows an SDS-PAGE gel of 3E8.scFv PEGylated with a 1.8 kD discrete PEG (Quanta BioDesign) at molar excesses of PEG to protein ranging from 6x to 20x. As shown, the number of PEGylated lysines within 3E8.scFv increases as the molar excess of PEG to protein increases. The mass spectrometry results showed that there were 9 PEGylated lysines between these samples: 36, 109, 146, 147, 193, 197, 208, and 2 residues within the linker (not shown in the PyMOL image). To summarize, the blue, orange, and red spheres in figure 18 are lysine residues identified as potentially problematic by the Magliery lab, by both the Magliery lab and the Wysocki Lab, and by only the Wyocki Lab, respectively.

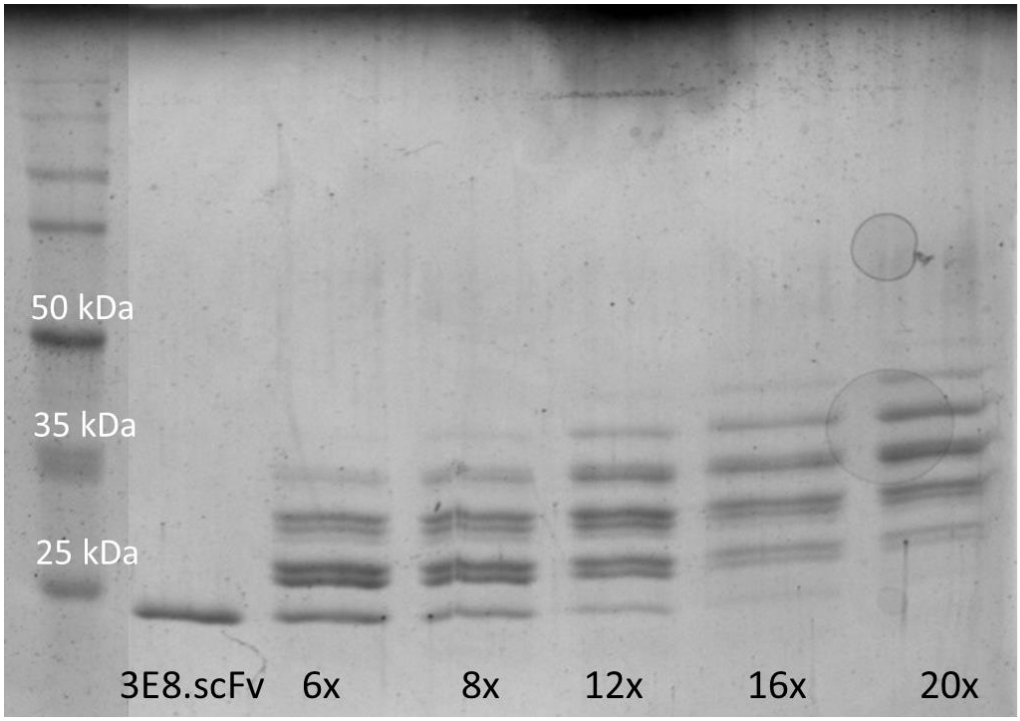

Figure 19. NHS-ester PEGylation of 3E8.scFv with 1.8 kD discrete PEG

4.1.2 Site-Directed Mutagenesis

In order to determine which lysine(s) is problematic, selected lysines in 3E8.scFv were systematically mutated to arginines, effectively eliminating PEGylation sites. Before PEGylated 3E8.scFv was sent for analysis by mass spectrometry, 5 mutants of 3E8.scFv, each containing a lysine replacement were engineered by site-directed mutagenesis: K24R, K36R, K157R, K193R, and K208R. Following mass spectrometry, 3 additional mutants of 3E8.scFv were engineered: K109R, K146/147R, and K197R. The amplified reassembly of the mutagenic fragments for each construct (shown in figure 20) was digested and ligated into the pHLIC plasmid, which was transformed into DH10B Competent cells. The DNA was purified from the cells after an overnight growth and sequence confirmed.

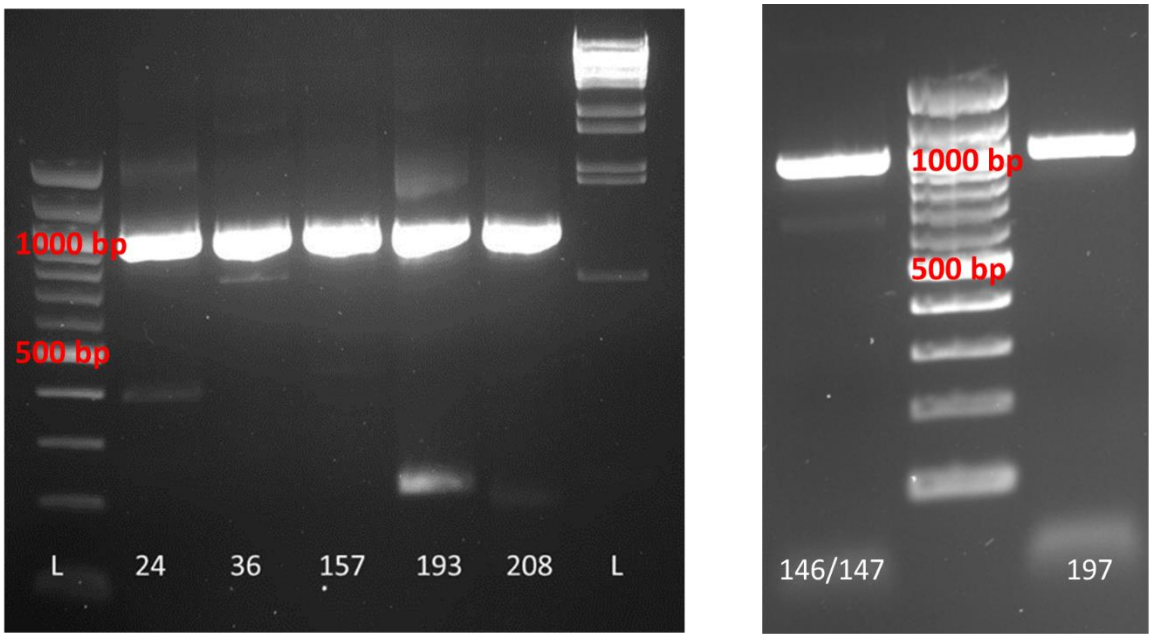

Figure 20. Amplified gene products for lysine to arginine constructs

In order to study the possibility of more than lysine being problematic for PEGylation at medium loads, two additional constructs were engineered. A mutant of 3E8.scFv called "penta 205C" was synthesized by Genewiz, Inc. (New Jersey, USA) that contained 5 lysine to arginine mutations (24, 36, 157, 193, and 208) and the 205C linker that is found in wild-

type 3E8.scFv. Furthermore, the mass spectrometry results indicated that 2 lysines within the 205C linker were also frequently PEGylated. A second construct, called "penta $(G_4S)_4$" was synthesized to address this issue. Penta $(G_4S)_4$ contains the same 5 mutations as penta 205C, in addition to the replacement of the 205C linker with a linker containing only glycines and serines. Once received, the genes were digested out of the pUC57 plasmid and ligated into pHLIC. Figure 21 shows multiple analytical digests of penta 205C and penta $(G_4S)_4$ with BamHI and NdeI. The presence of the ~900 bp band indicates that the ligations of the genes into pHLIC were successful. These genes were sequence confirmed.

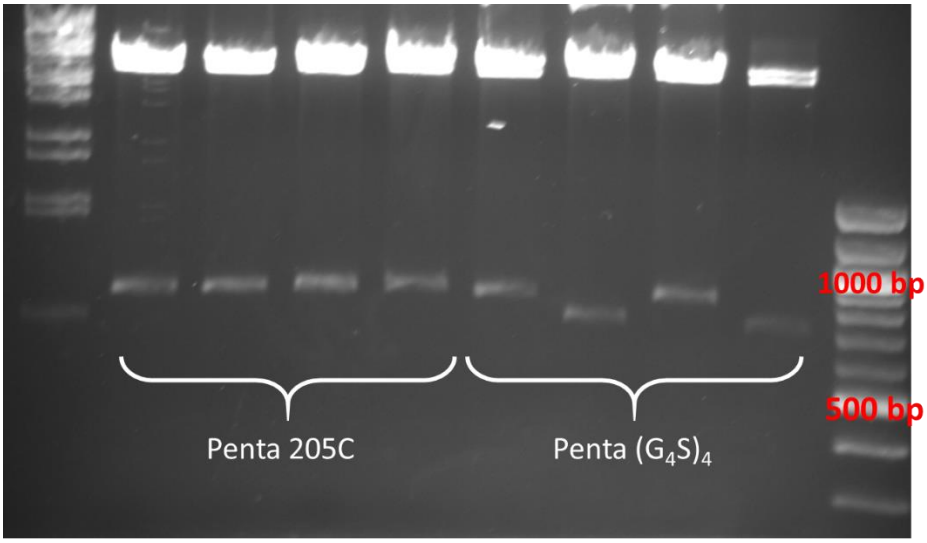

Figure 21. Analytical digests of penta 205C and penta $(G_4S)_4$

4.2 Expression and Purification of 3E8.scFv Constructs

All of the 3E8.scFv constructs were expressed in the same conditions and purified using the same techniques, with the exception of K146/147R, K197R, penta 205C, and penta $(G_4S)_4$. First, the proteins were expressed in C43(DE3) cells, the cells were lysed, and the proteins were purified from the cell lysate using affinity chromatography with the protein L column. Then, the histidine-tag was cleaved off using TEV protease, and ion exchange

chromatography with the Resource S column was used to remove the histidine-tag and TEV protease from the cleaved protein. Figures 22-29 show the elution profiles from ion exchange for 3E8.scFv (wild-type), K24R, K36R, K157R, K193R, K208R, 3E8.scFv.Cys, and 3E8.scFv.FLAG. The red line indicates the concentration of ion exchange buffer B. Fractions from ion exchange containing the purified protein were combined. K146/147R and K197R do not have ion exchange profiles because they were not purified by ion exchange after TEV cleavage, but rather by nickel column affinity purification. In these cases, the TEV cleaved proteins were collected in the flow-through of the nickel column because they no longer contained the histidine tag. Penta 205C and penta $(G_4S)_4$ were synthesized without histidine tags, so they were not TEV cleaved and thus ion-exchange was not needed.

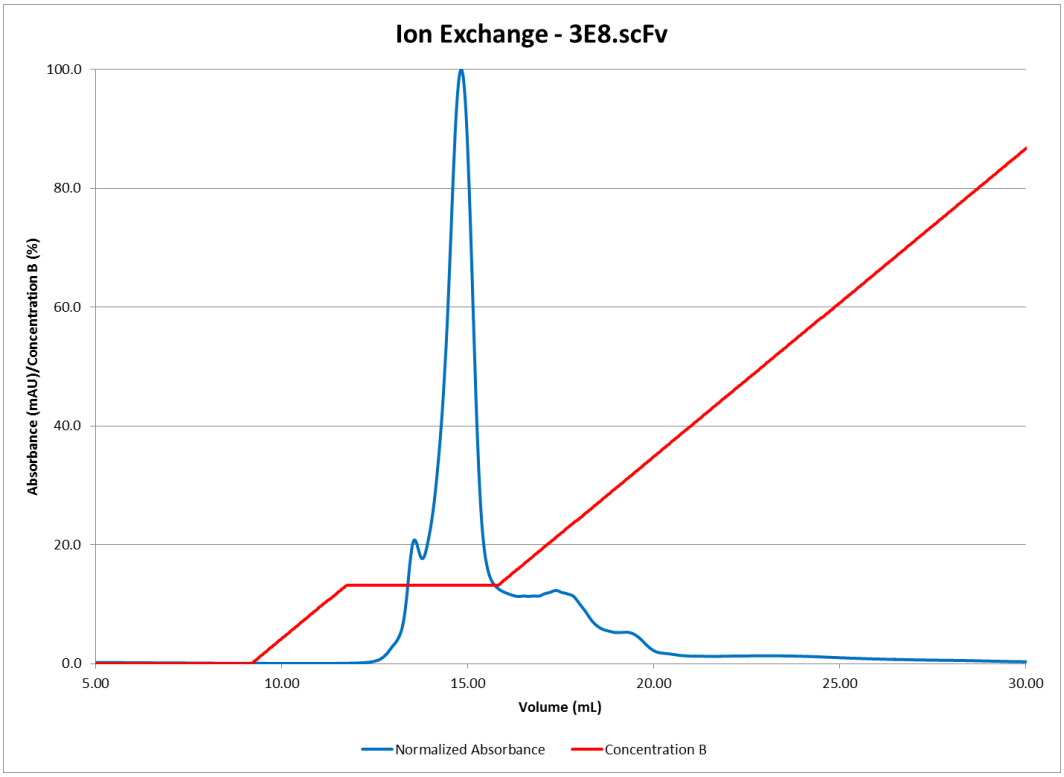

Figure 22. Ion exchange elution profile for 3E8.scFv

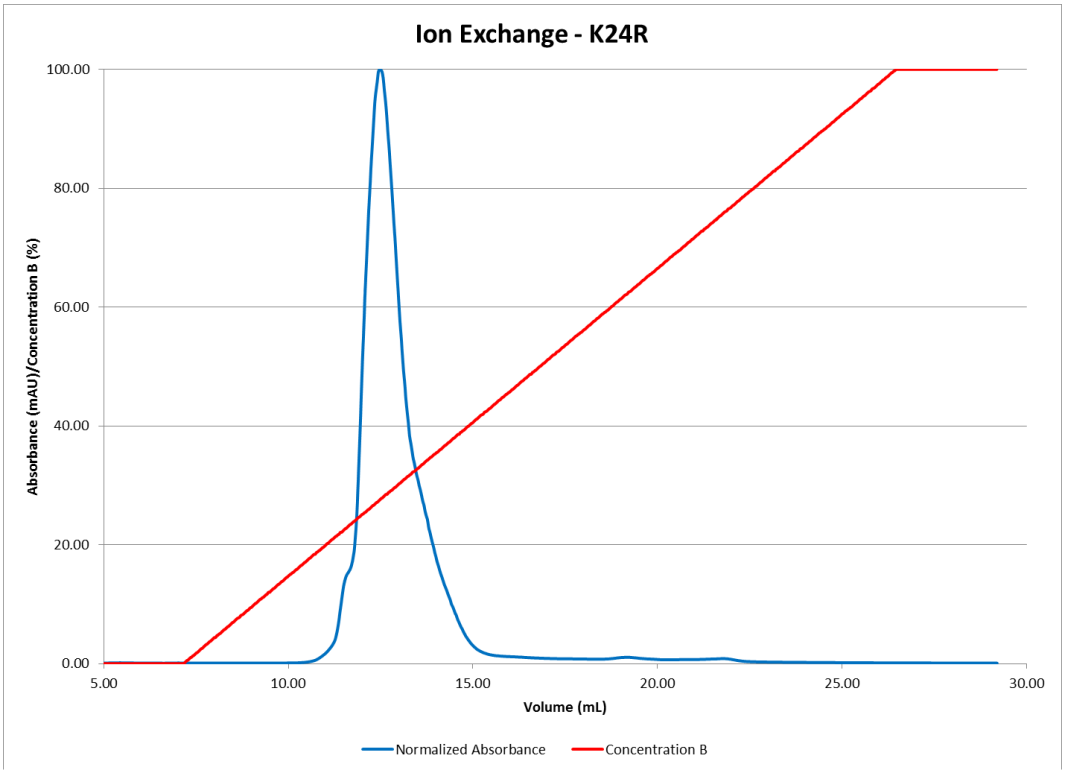

Figure 23. Ion exchange elution profile for K24R

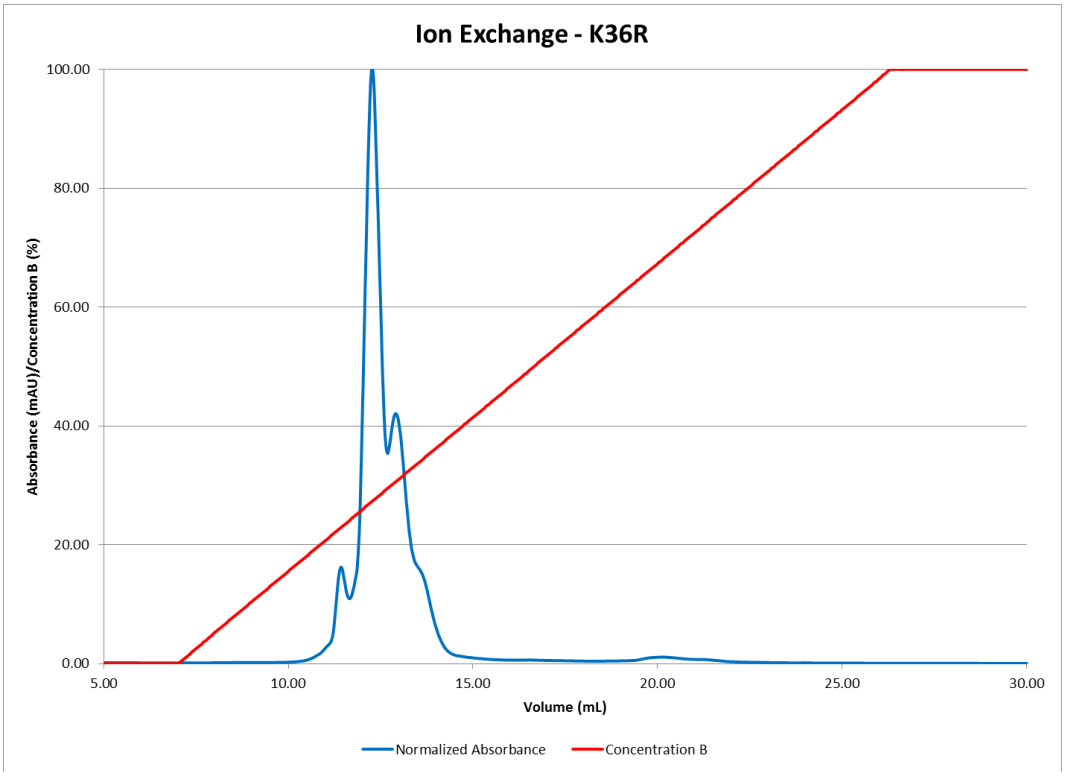

Figure 24. Ion exchange elution profile for K36R

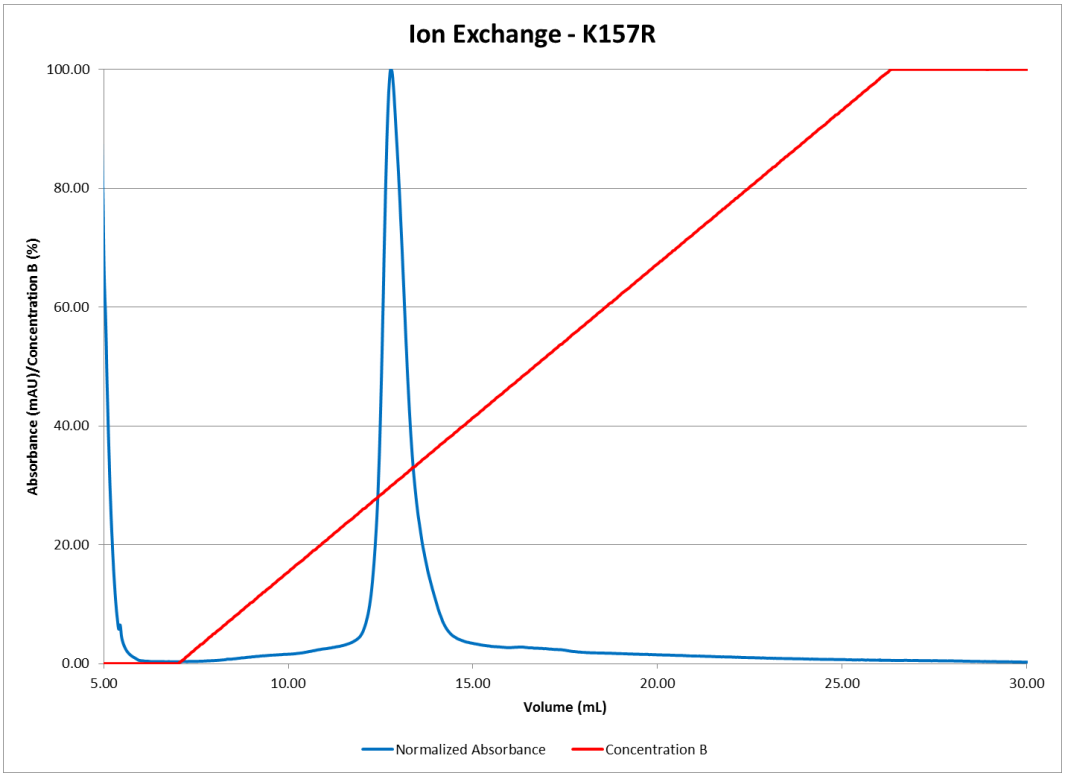

Figure 25. Ion exchange elution profile for K157R

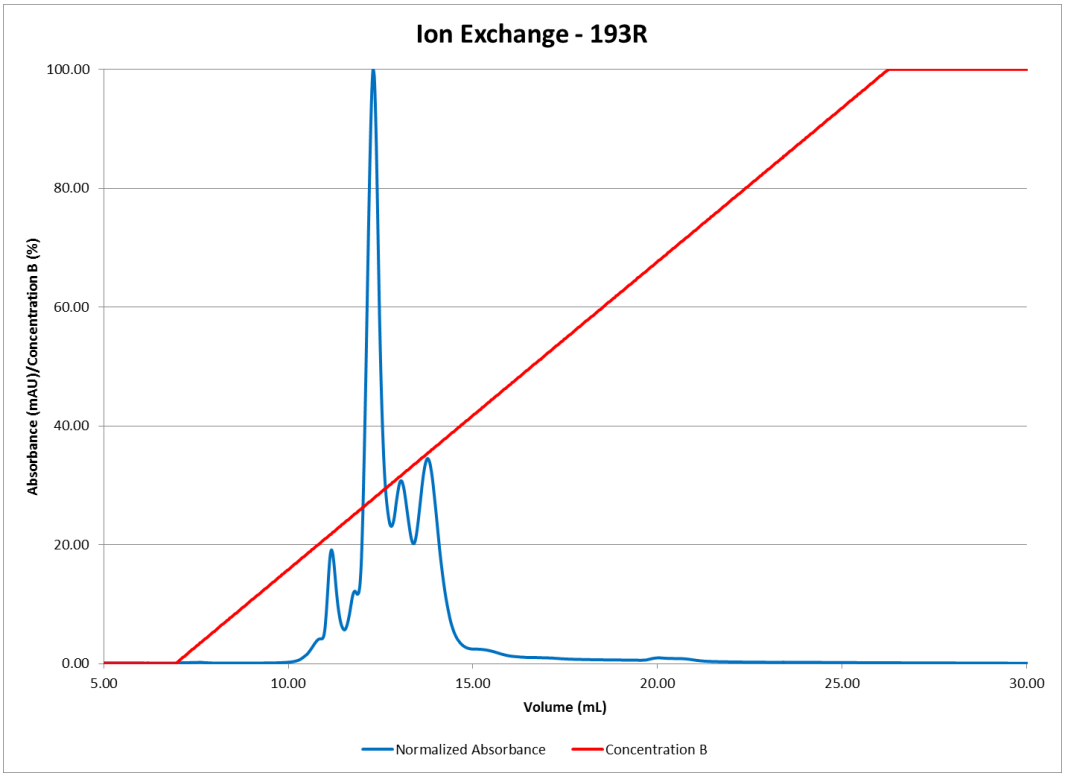

Figure 26. Ion exchange elution profile for K193R

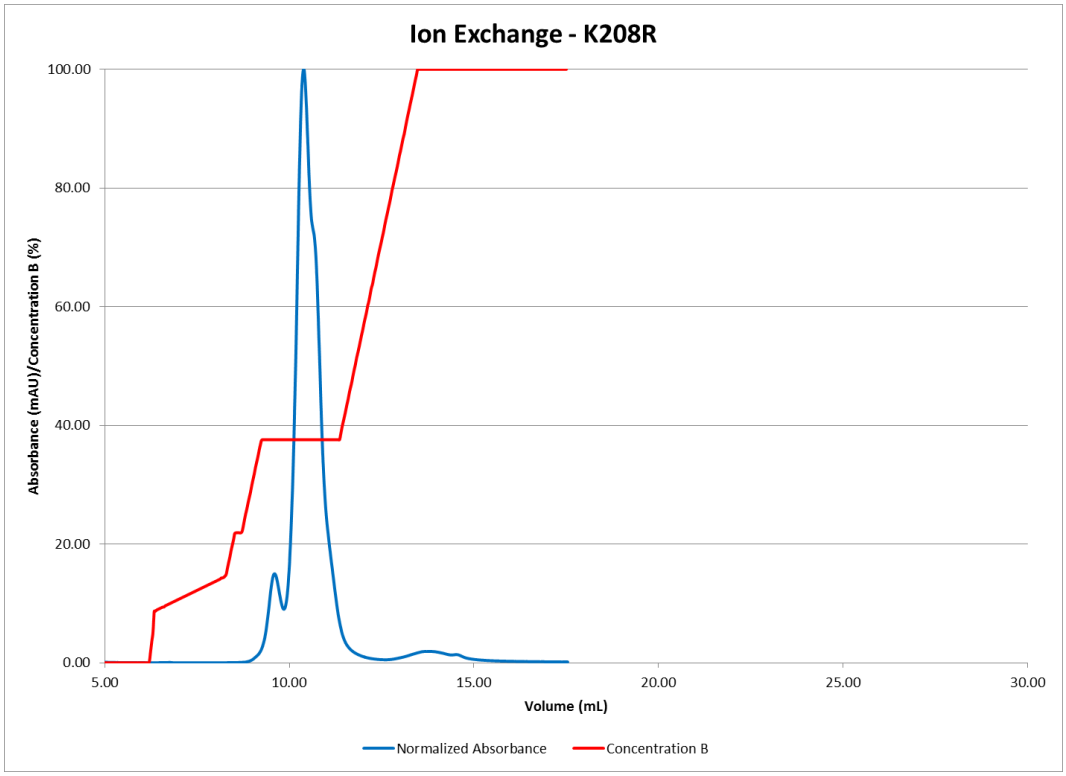

Figure 27. Ion exchange elution profile for K208R

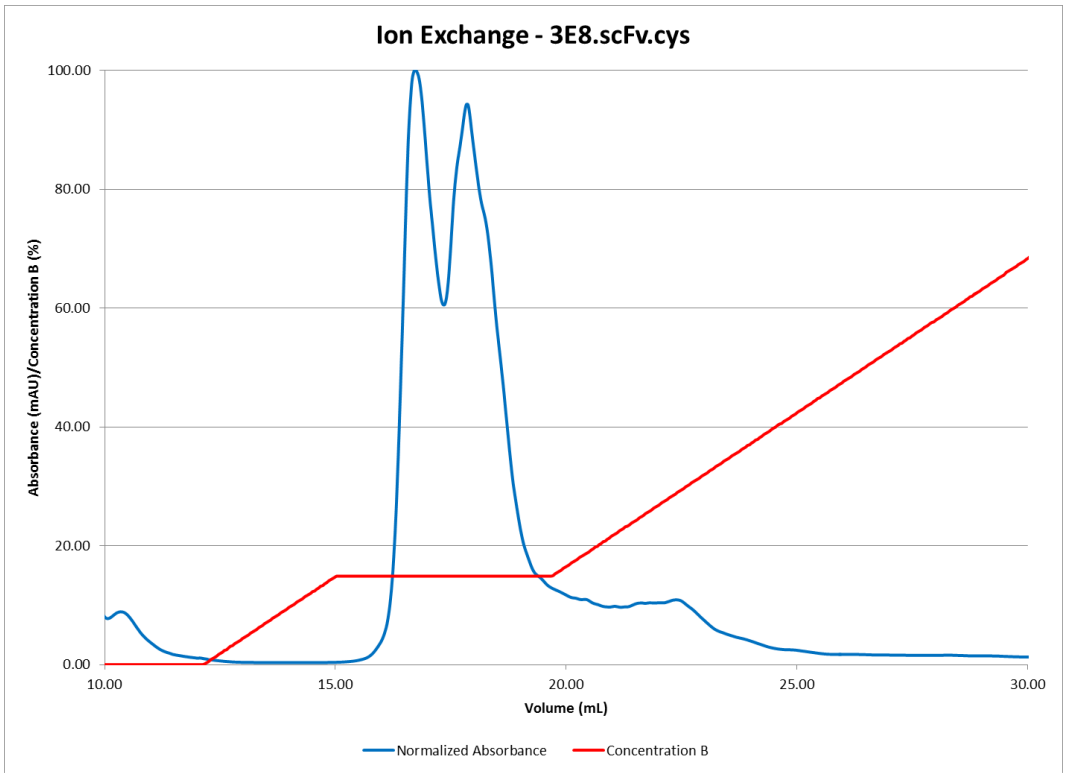

Figure 28. Ion exchange elution profile for 3E8.scFv.cys

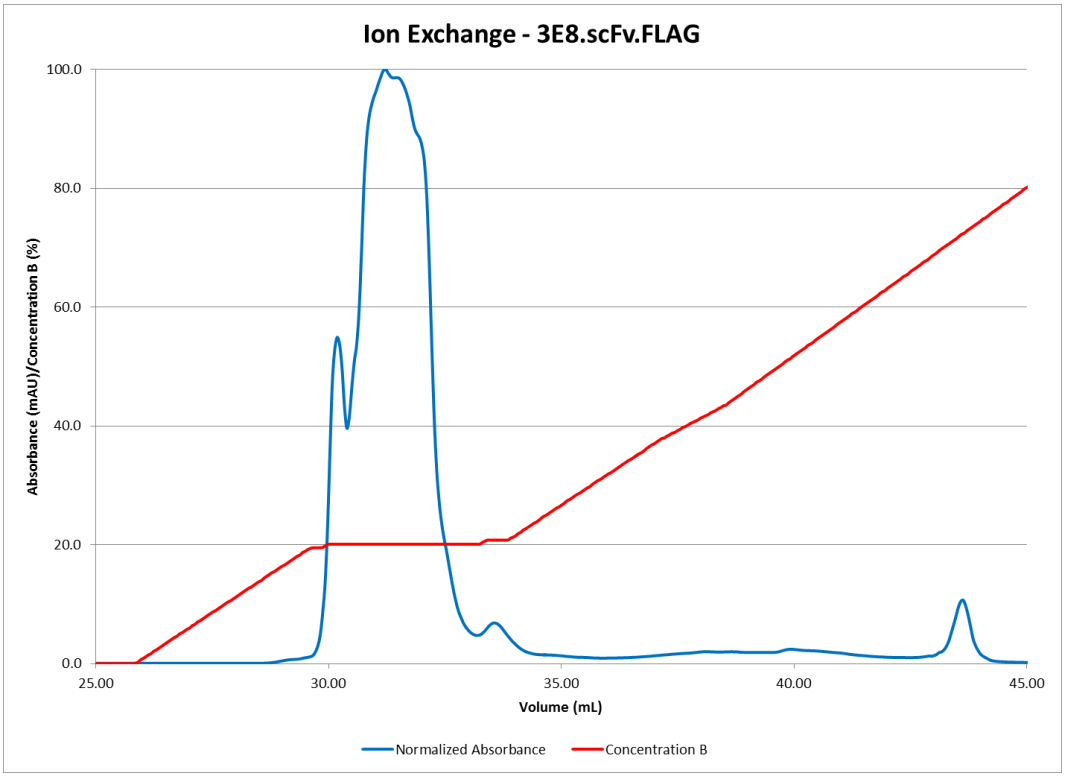

Figure 29. Ion exchange elution profile for 3E8.scFv.FLAG

Figure 30 shows an SDS-PAGE gel of the 3E8.scFv lysine to arginine constructs after affinity chromatography purification by the protein L column, TEV cleavage, and ion exchange chromatography. Based on the gel, it appears that the expression and purification resulted in good yields for all constructs except for 157 and penta 205C. In fact, this same result was seen after repeated purifications of these two constructs. Additionally, the smaller band that exists in some of the constructs towards the bottom of the gel is believed to be proteolysis product. Nonetheless, the samples look relatively pure and contain only a small of amount of proteolysis products. The characterization and PEGylation of these constructs will be discussed in section 4.3. (K109R is in the process of production.)

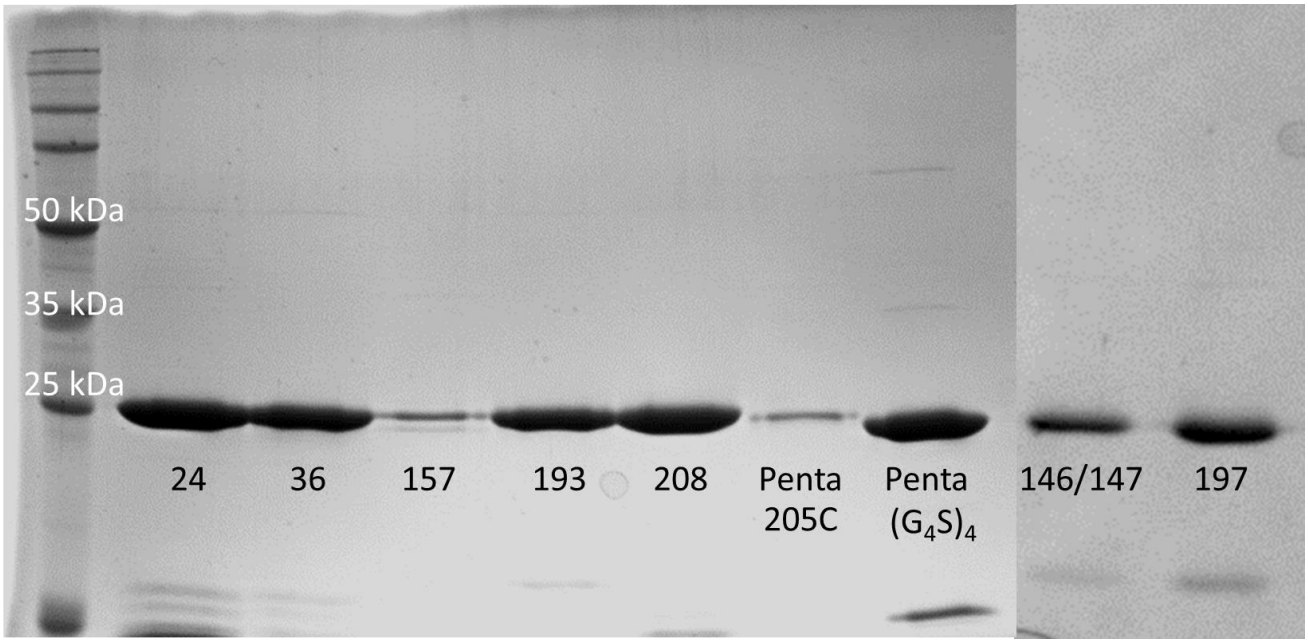

Figure 30. Lysine to arginine constructs after cytoplasmic purification and TEV cleavage

Figures 31, 32, and 33 show the purifications of 3E8.scFv, 3E8.scFv.FLAG, and 3E8.scFv.Cys, respectively. All three of these constructs appear to be very pure with small amounts of proteolysis product in 3E8.scFv and 3E8.scFv.Cys.

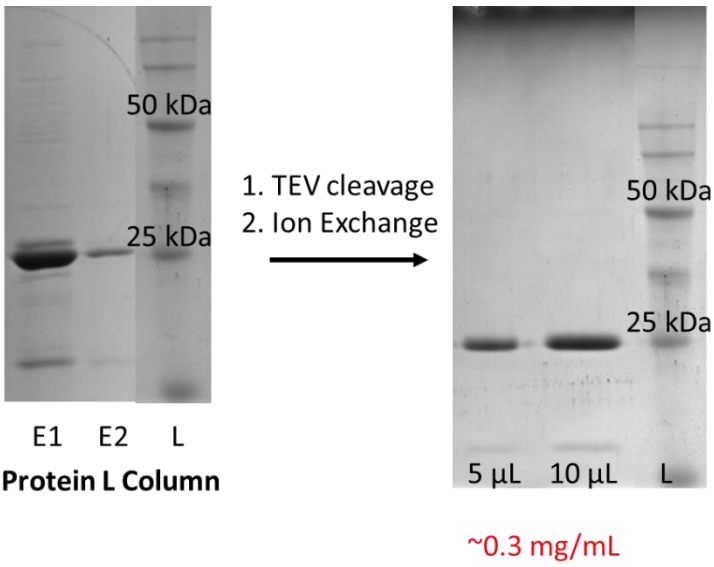

Figure 31. 3E8.scFv after cytoplasmic purification and TEV cleavage

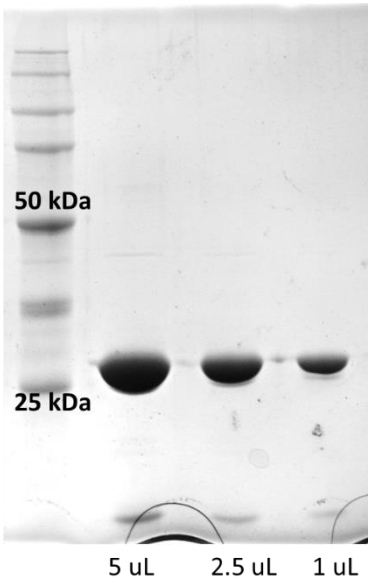

Figure 32. 3E8.scFv.FLAG after cytoplasmic purification and TEV cleavage

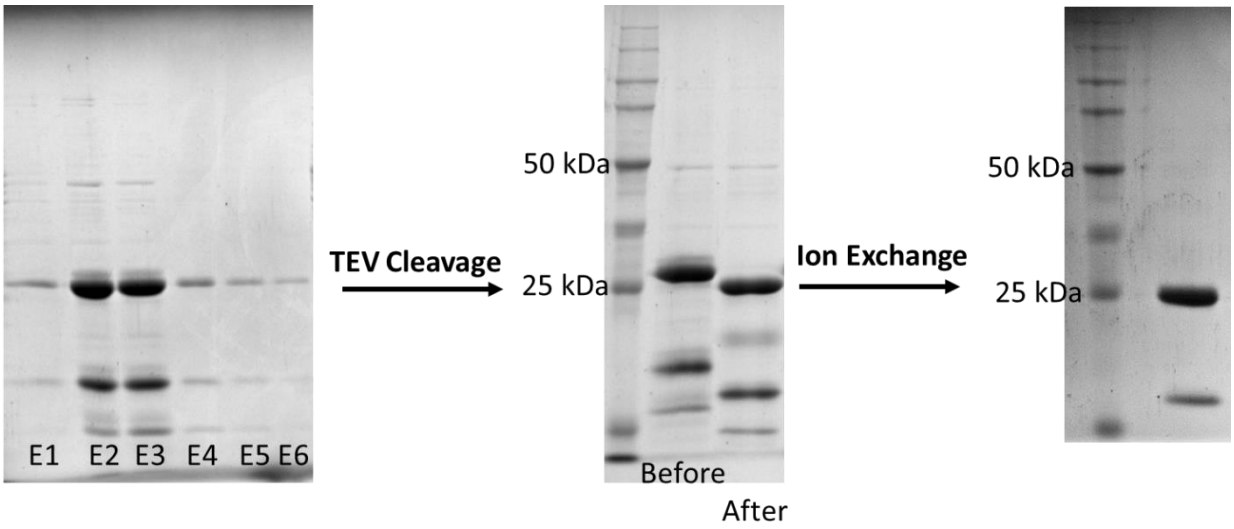

Figure 33. Cytoplasmic purification of 3E8.scFv.cys

4.3 Non-Specific PEGylation at Lysines and Characterization

The ultimate goal of this project is to create a mutant of 3E8.scFv with equal or better binding affinity and stability as 3E8.scFv after PEGylation by NHS-ester chemistry. In order to study the effect of the mutation(s) on the biophysical properties of 3E8.scFv, differential scanning fluorimetry (DSF) and surface plasmon resonance (SPR) were performed for each construct. Figure 34 shows the normalized melting curves obtained from DSF for each of the unPEGylated lysine to arginine mutants. The black line represents unPEGylated wild-type 3E8.scFv(205C). While some of the constructs were slightly destabilized, all of the constructs have melting temperatures within about 3 °C of wild-type 3E8.scFv(205C). The peak seen consistently around 55 °C for some of the samples is hypothesized to be from proteolysis product.

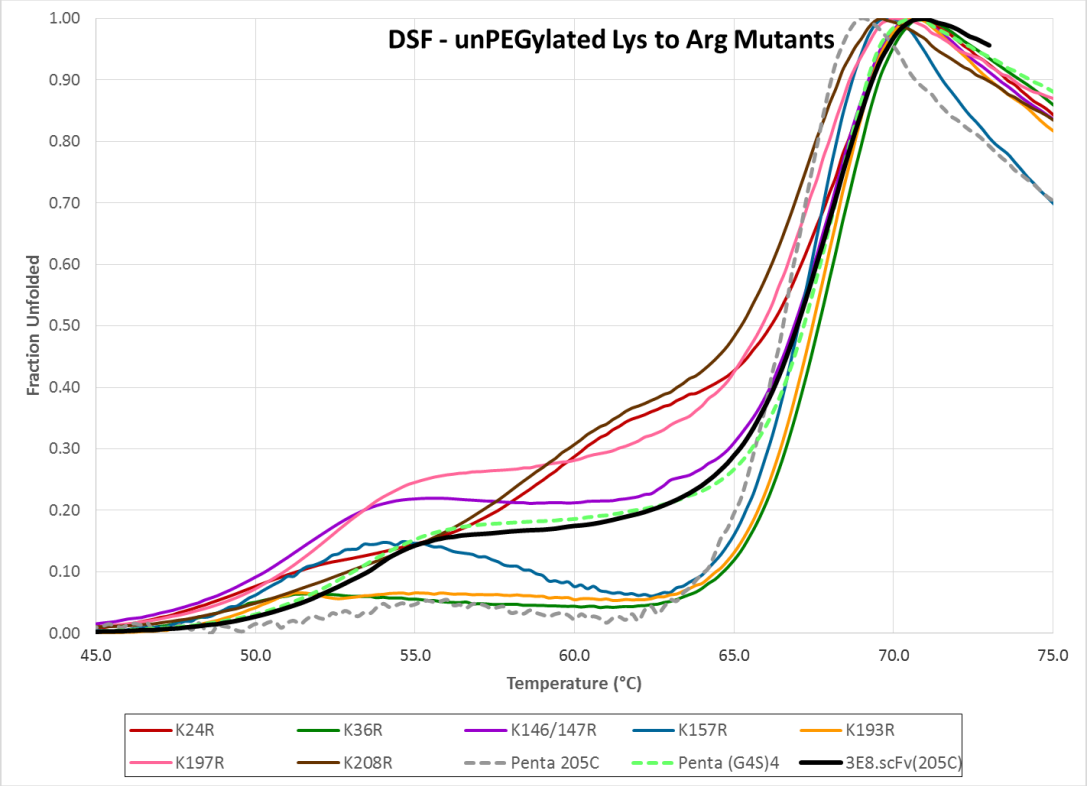

Figure 34. Melting curves for unPEGylated lysine to arginine constructs

Table 2 shows the dissociation constant (K_D) for each of the unPEGylated lysine to arginine constructs, which represents the dissociation between the antibody and the anitgen (TAG-72). Therefore, a smaller K_D indicates tighter binding to the target. Each of the single mutants retained its binding, while penta $(G_4S)_4$ lost some of its binding and was not further characterized.

Construct	K_D
3E8.scFv	12 nM
K24R	12.4 nM
K36R	11.6 nM
K157R	8.6 nM
K193R	11.8 nM
K208R	12.8 nM
Penta (G4S)4	236 nM

Table 2. K_D values for unPEGylated lysine to arginine constructs

Following the initial characterization of the unPEGylated lysine to arginine mutants, each of the single mutants was PEGylated at 16x excess (PEG to protein), the “medium load” of PEGylation which ablated binding and decreased thermal stability of 3E8.scFv(205C) in the preliminary studies. The non-specific PEGylation of the single mutants with a 1.8 kD discrete PEG (Quanta BioDesign) using NHS-ester chemistry is shown in figure 35. Every construct except K157R appears to have been successfully PEGylated to about the same degree. K157R was most likely PEGylated but is too faint to clearly see on the gel.

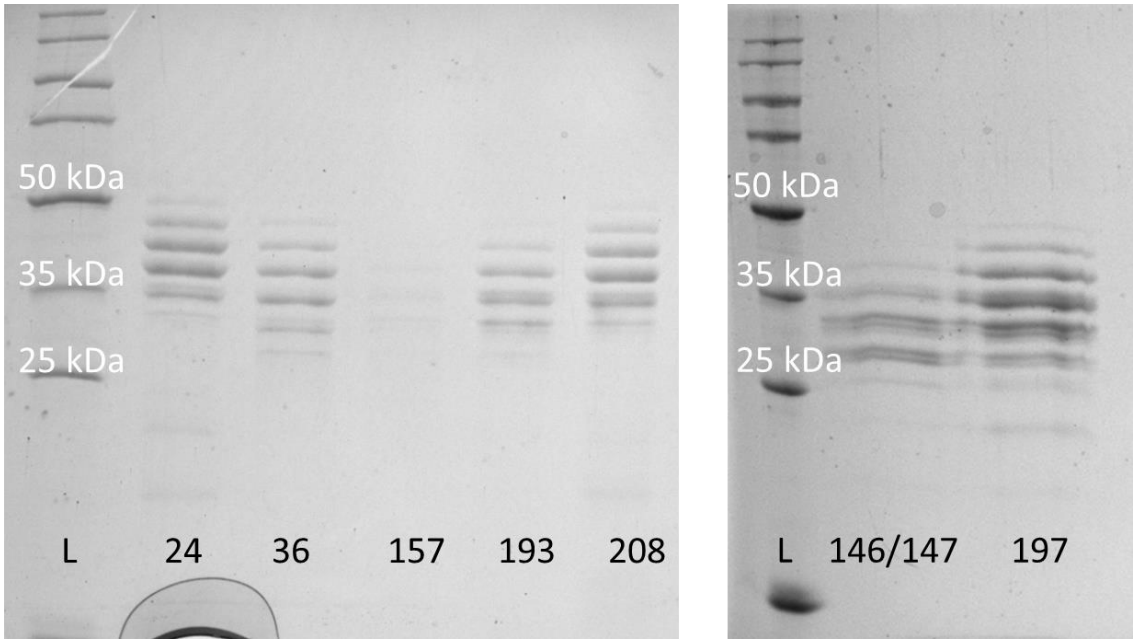

Figure 35. NHS-ester PEGylation of lysine to arginine constructs with 1.8 kD discrete PEG

Each of the PEGylated single mutants was characterized using DSF and SPR, similar to the unPEGylated mutants. Figure 36 shows the normalized melting curves obtained from DSF for the PEGylated single mutants. Again, the black line represents unPEGylated 3E8.scFv(205C) for reference. Similar to the results of the preliminary studies, these

constructs were slightly destabilized after 16x excess PEGylation, with the most stable constructs appearing to be K193R, K146/147R, and K36R.

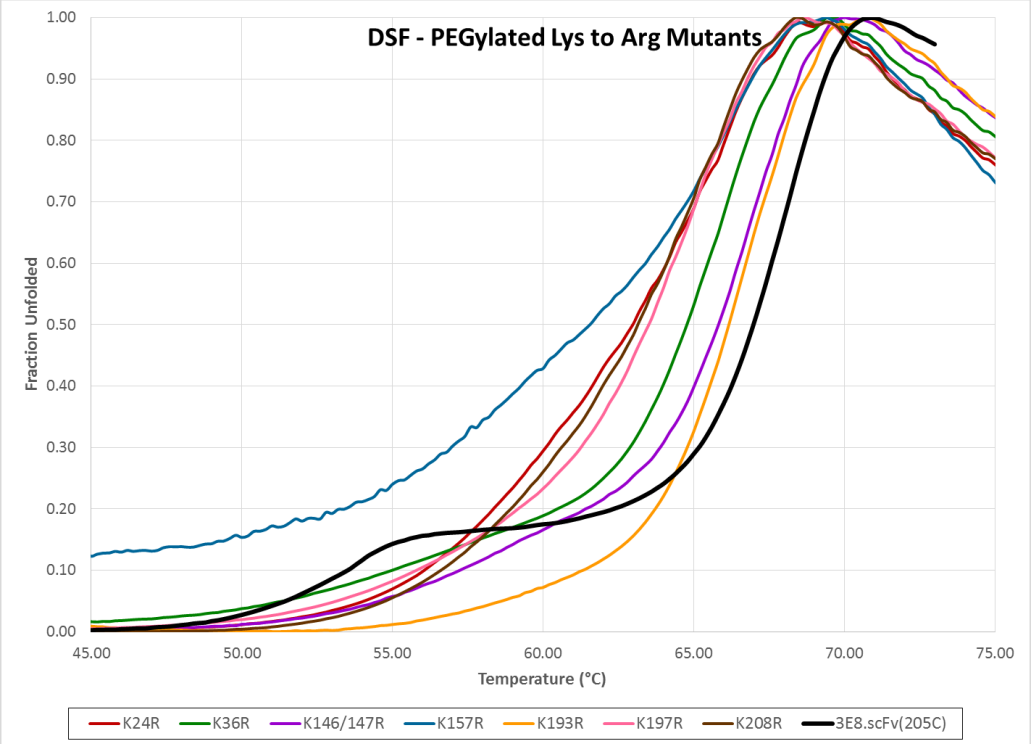

Figure 36. Melting curves for NHS-ester PEGylated lysine to arginine constructs

Table 3 shows the K_D values for 4 of the 7 PEGylated single mutants. SPR for PEGylated K146/147R, K157R, and K197R is currently in progress. While the binding affinity has decreased for each of the constructs shown here, the best binding constructs after PEGylation are K24R and K208R. Compared to the >1 µM binding constant for PEGylated 3E8.scFv, K24R and K208R have greatly improved binding affinity to TAG-72.

PEGylated Construct	K_D
3E8.scFv	> 1 µM
K24R	72.2 nM
K36R	848 nM
K193R	1608 nM
K208R	49.9 nM

Table 3. K_D values for NHS-ester PEGylated lysine to arginine constructs

4.4 Specific PEGylation at Cysteines and Characterization

To study the possibility and effects of PEGylation at a single site in 3E8.scFv, a mutant of 3E8.scFv called 3E8.scFv.Cys containing a C-terminal cysteine was PEGylated using maleimide chemistry. Three linear PEGs of sizes 5 kD, 20 kD, and 40 kD and one branched Y-shaped PEG of size 40 kD were used for this experiment. The difference in shape between a linear and branched PEG is shown in Figure 37.

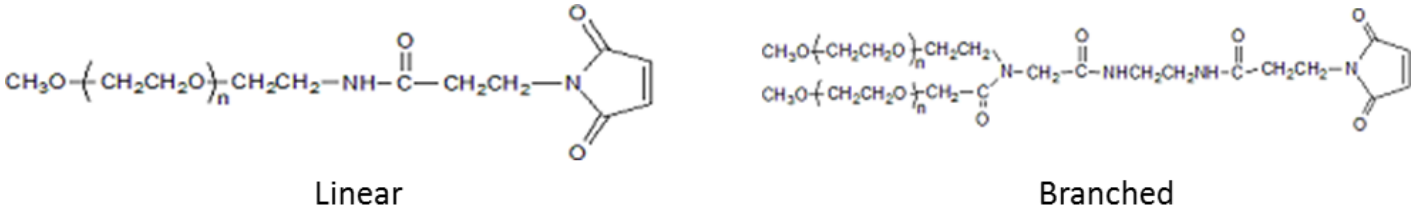

Figure 37. Structures of linear and branched maleimide-activated PEGs

Four separate samples of 3E8.scFv.Cys were PEGylated overnight at a 50x molar excess of PEG to protein. To remove any non-PEGylated protein and the PEG itself, cation exchange chromatography was used. The elution profiles of each of the PEGylated samples are shown in figures 38-41. The red line represents the concentration of ion exchange buffer B at the time of the elution. Once the elution fractions were analyzed by SDS-PAGE, any elutions containing the purified protein were combined and dialyzed into PBS for characterization.

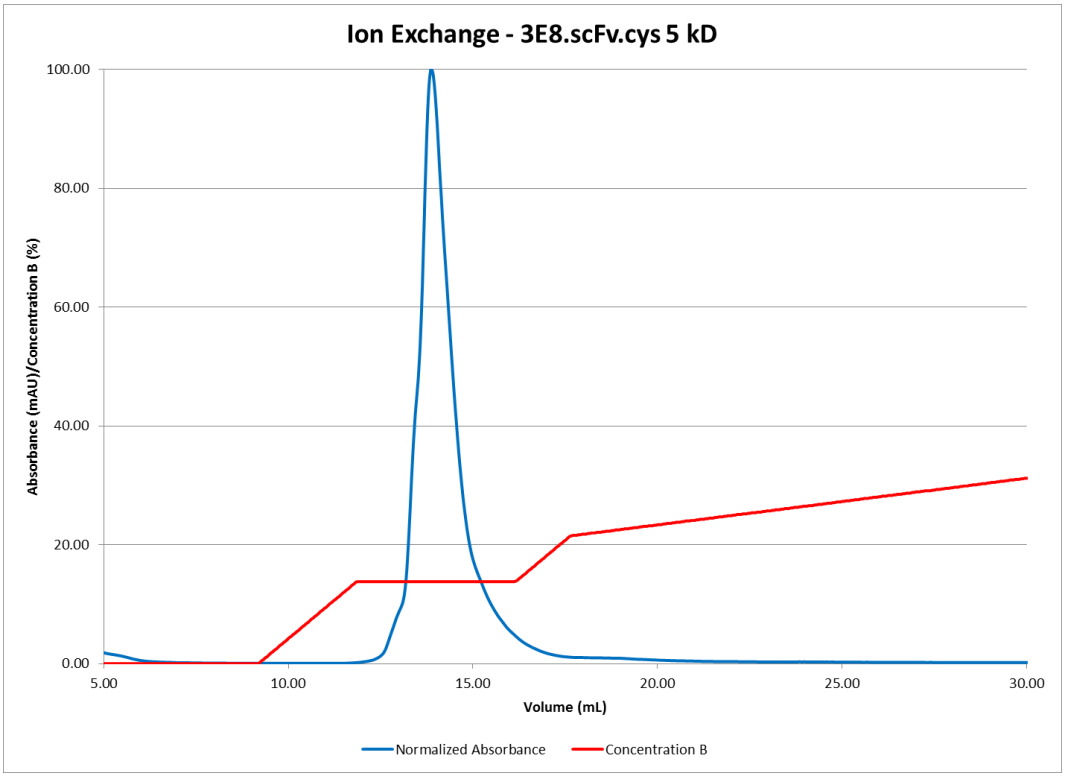

Figure 38. Ion exchange elution profile of 5 kD PEGylated 3E8.scFv.Cys

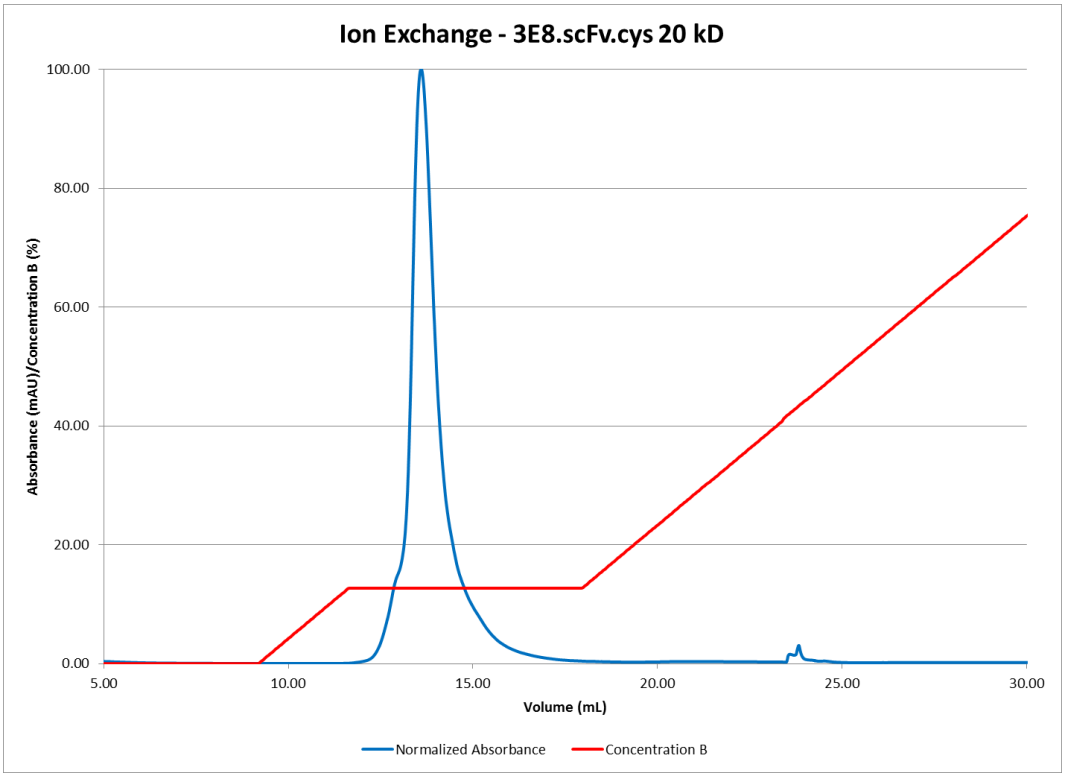

Figure 39. Ion exchange elution profile of 20 kD PEGylated 3E8.scFv.Cys

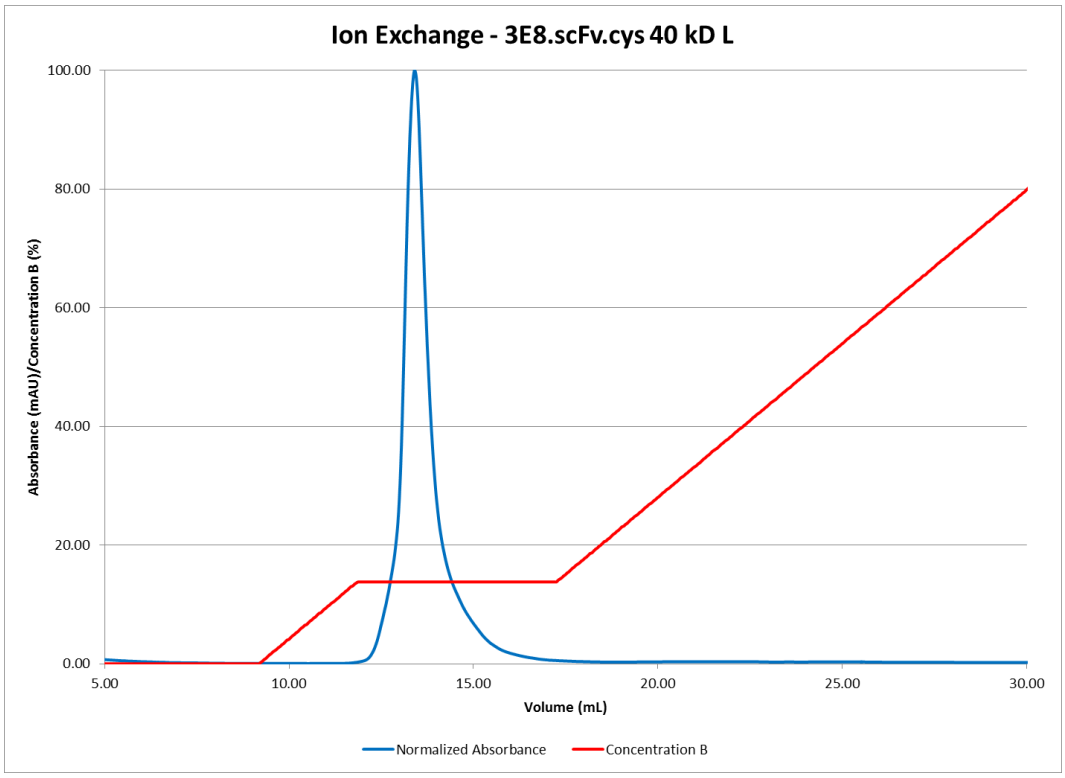

Figure 40. Ion exchange elution profile of 40 kD L PEGylated 3E8.scFv.Cys

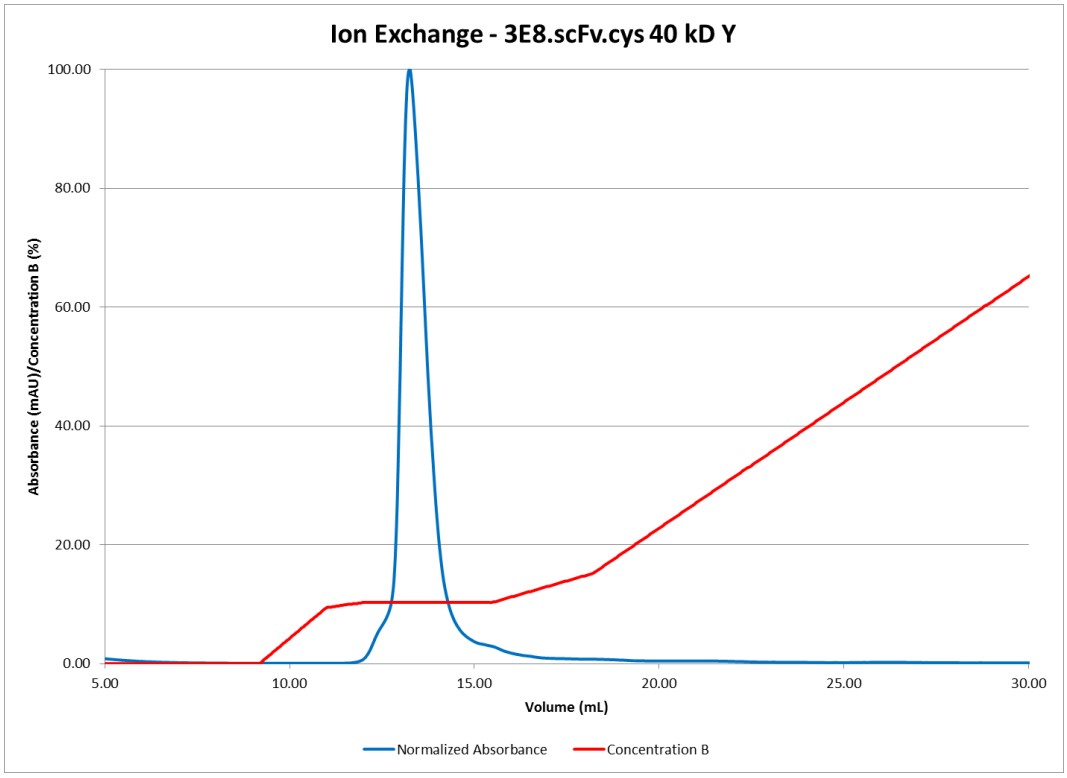

Figure 41. Ion exchange elution profile of 40 kD Y PEGylated 3E8.scFv.Cys

Figure 42 shows an SDS-PAGE gel of the ion-exchange purified PEGylated 3E8.scFv.Cys samples after dialysis into PBS buffer. Each of the samples looks very pure with a small amount of proteolysis product towards the bottom of the gel.

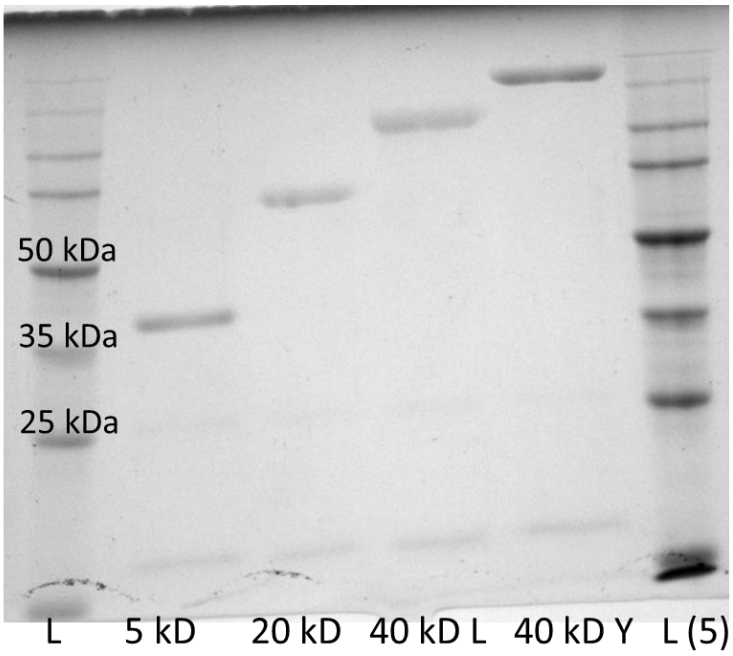

Figure 42. Maleimide PEGylated 3E8.scFv.cys samples after ion exchange purification

Gel filtration was performed on each of these samples, in addition to unPEGylated 3E8.scFv.Cys. 200 µL of sample was run over a 25 mL Superdex 75 10/300 GL size exclusion chromatography column (GE Healthcare Life Sciences) at a constant flow rate. The elution profile, shown in figure 43, agrees with what one might expect based solely on the sizes of the PEGs. Protein conjugated to a larger PEG elutes from the column faster than protein conjugated to a smaller PEG. The results also indicate that each of the samples exists solely as monomers. The peak at ~11.70 mL, which exists in every sample except 40 kD Y, may be from proteolysis product that was previously mentioned.

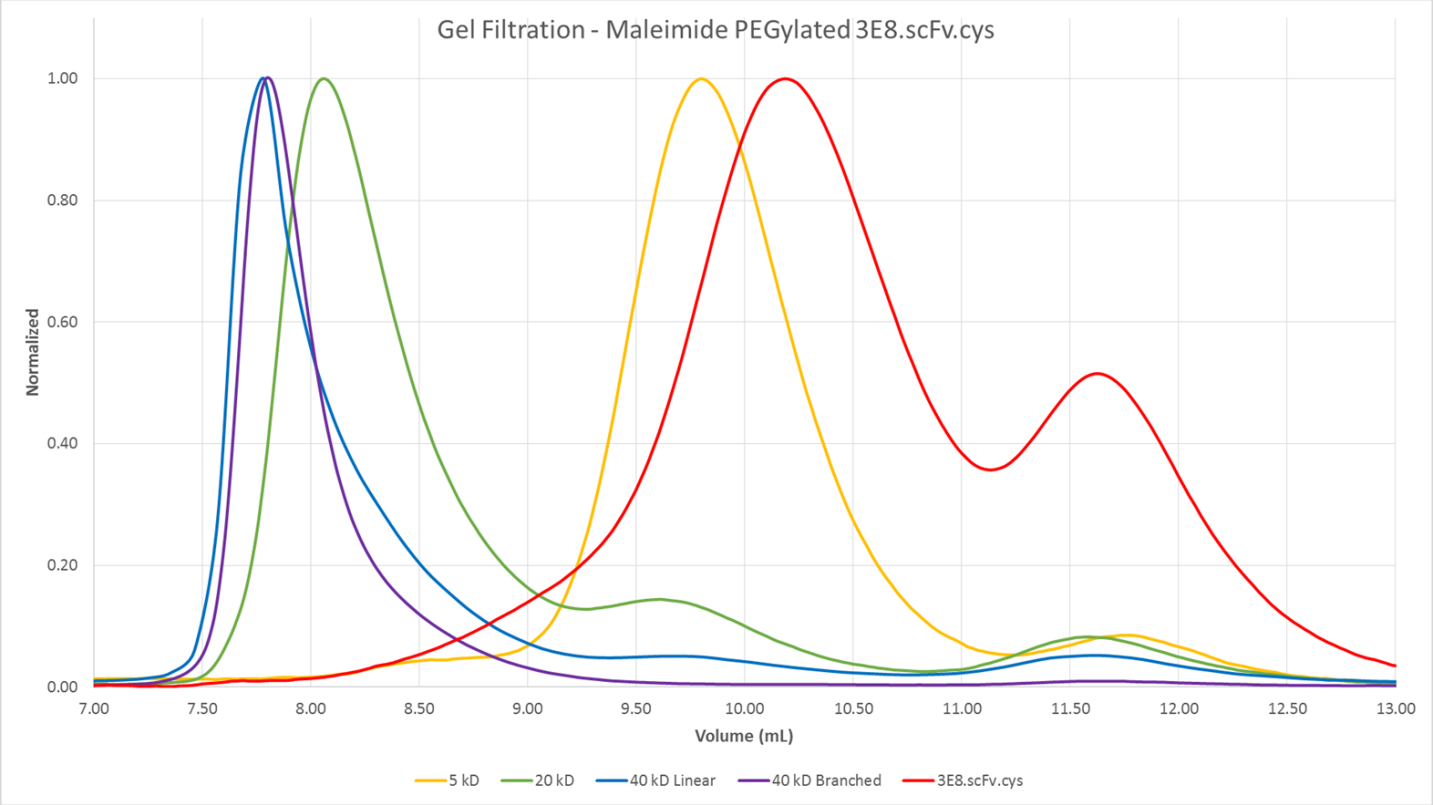

Figure 43. Gel filtration elution profiles of PEGylated 3E8.scFv.Cys samples

The melting curves obtained from DSF for the PEGylated 3E8.scFv.Cys samples are shown in figure 44. The black line represents 3E8.scFv(205C) for comparison, while the colored lines indicate 3E8.scFv.Cys and the PEGylated samples. These results show not only that 3E8.scFv.Cys has an extremely similar melting point as 3E8.scFv(205C) but also that 3E8.scFv.Cys is not destabilized by maleimide-activated conjugated to both small and large PEGs. The smaller peak at ~52 °C may be of proteolysis product.

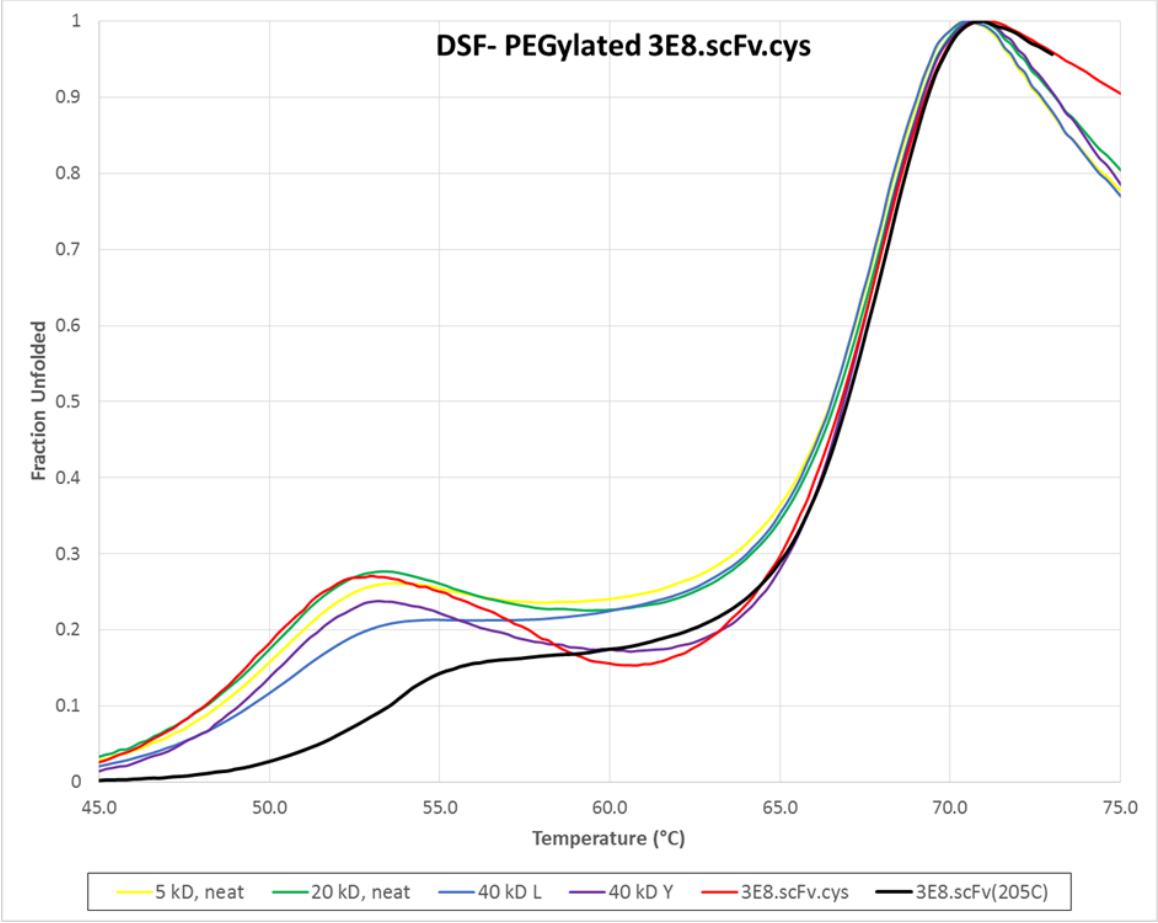

Figure 44. Melting curves of PEGylated 3E8.scFv.Cys samples

The binding affinity of each sample to TAG-72 was analyzed by SPR, the results of which are shown in table 4. 3E8.scFv.Cys has slightly decreased binding compared to 3E8.scFv(205C) but appears to retain its binding after maleimide PEGylation. Also, conjugation to larger PEGs seems to disrupt binding slightly more than smaller PEGs.

Construct	K_D
3E8.scFv.cys	39 nM
5 kD	26 nM
20 kD	20 nM
40 kD L	33 nM
40 kD Y	39 nM

Table 4. K_D values for Maleimide PEGylated 3E8.scFv.Cys constructs

4.5 Optimization of 3E8.scFv.FLAG for Immunohistochemistry

To first determine whether 3E8.scFv.FLAG binds to TAG-72, the scheme illustrated in figure 45, which is a simplified version of the one shown in figure 16, was tested using a Western blot. After the purification of 3E8.scFv.FLAG, each of the steps of the purification was run on a SDS-PAGE gel. The contents of the gel was transferred to a nitrocellulose membrane, which was stained with a 1:1000 dilution of anti-FLAG HRP conjugate (Sigma Aldrich) overnight and DAB/H_2O_2. The results, shown in figure 46, indicate that the anti-FLAG HRP conjugate binds to 3E8.scFv.FLAG, which is found in the 1 µL and 10 µL elution lanes.

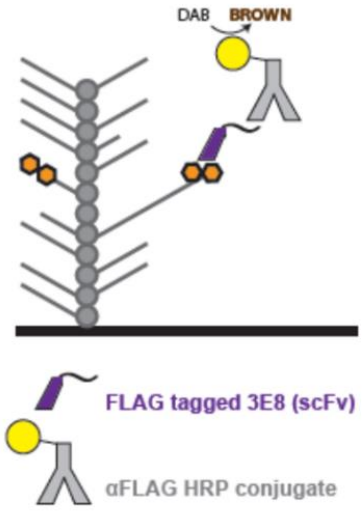

Figure 45. IHC scheme of 3E8.scFv.FLAG with anti-FLAG HRP conjugate

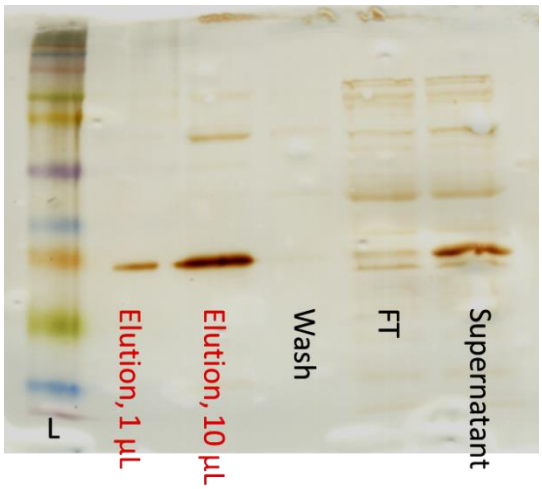

Figure 46. Western blot with anti-FLAG HRP conjugate

After the success of the western blot, a dot blot was performed using the same chemistry. However, this time, bovine submaxillary mucin (which contains TAG-72) was first spotted onto the corner of the nitrocellulose. The membrane was incubated with 1 mg/mL, 0.1 mg/mL, and 0.5 mg/mL 3E8.scFv.FLAG and a 1:5000 dilution of anti-FLAG

HRP conjugate for 1 hour, and then developed with DAB/H_2O_2. A negative control was done alongside by replacing 3E8.scFv.FLAG with PBS buffer. The results are shown in figure 47 and indicate very good staining where the antigen was spotted with almost no background staining after the immediate addition of DAB.

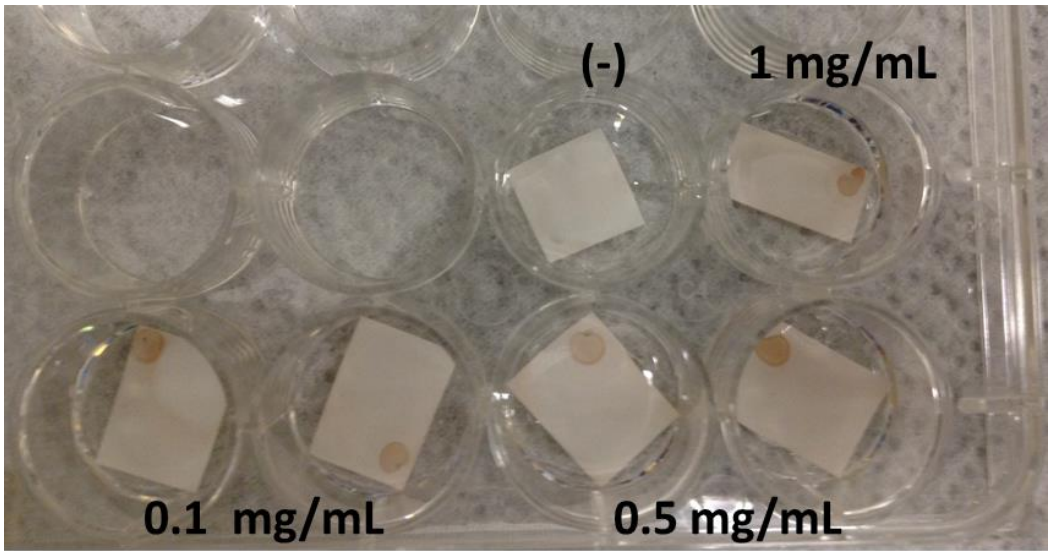

Figure 47. Dot blots with anti-FLAG HRP conjugate

To possibly improve the signal and sensitivity of the staining, an additional step was added to the scheme described above. As shown in below in figure 48, the anti-FLAG HRP conjugate was replaced with the anti-FLAG Biotin conjugate and a tertiary agent (streptavidin HRP conjugate) was added. A Western blot to test this chemistry was performed with 3E8.scFv.FLAG, 1:1000 dilution of anti-FLAG biotinylated (Thermo Scientific) overnight at 4 °C, VECTASTAIN (Vector Laboratories) for 1 hour at RT, and DAB/H_2O_2. VECTASTAIN was prepared by adding 1 drop of Reagent A and 1 drop of Reagent B to 3 mL of PBS buffer. The results are shown in figure 49 and indicate a very strong staining for the band of 3E8.scFv.FLAG on the nitrocellulose paper.

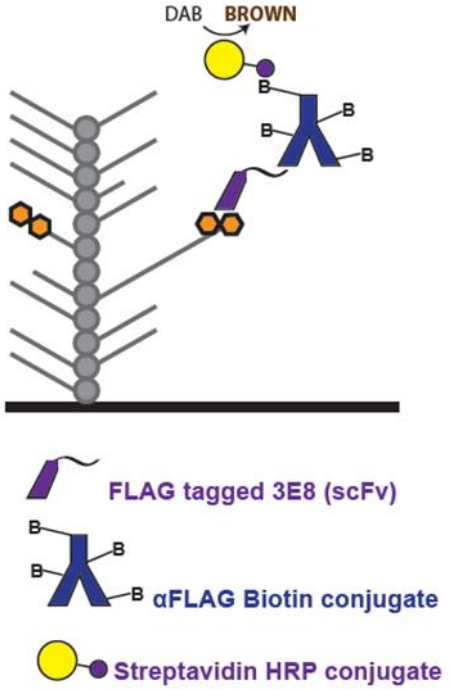

Figure 48. IHC scheme of 3E8.scFv.FLAG with anti-FLAG Biotin conjugate

Figure 49. Western blot with anti-FLAG Biotin conjugate and VECTASTAIN

The scheme with the anti-FLAG Biotin conjugate and VECTASTAIN was further studied with a dot blot. 3E8.scFv.FLAG was spotted onto the corner of nitrocellulose paper and developed with a 1:1000 dilution of anti-FLAG Biotin conjugate at RT, VECTASTAIN for 2 hours at RT, and DAB/H_2O_2. Images of the results were not recorded; however, the dot blot was as successful as the Western blot shown in figure 49. The blotted corner of nitrocellulose stained dark brown with little background staining.

Chapter 5: Conclusions and Future Directions

Mass spectrometry of non-specifically PEGylated 3E8.scFv showed that many surface lysines within the protein were PEGylated. To pinpoint which lysines were potentially problematic to binding affinity and stability, these lysines were systematically mutated to arginines, thus creating numerous variants of 3E8.scFv. With the exception of two variants (K157R and penta 205C), each variant was expressed and purified to give produce great yields. These variants were characterized before PEGylation and it was determined that the variants containing only a single lysine to arginine mutation retained their binding affinity to TAG-72 and were only slightly destabilized. Following non-specific PEGylation, the melting curves of the PEGylated samples showed that they were again destabilized, with some constructs showing larger destabilization than others. More interestingly, two of the constructs (K24R and K208R) retained their binding affinity after PEGylation, thereby indicating that the 24 and 208 lysines may be responsible for the ablation of binding seen after the PEGylation of wild-type 3E8.scFv. Further analysis of the binding affinity of K109R, K146/147R, and K197R may determine if these residues are also problematic for non-specific PEGylation. It is possible that the most stable and best binding version of non-specifically PEGylated 3E8.scFv will have multiple lysine to arginine replacements. Thus, it would be interesting to engineer and characterize a variant of 3E8.scFv with mutations only to the 24 and 208 lysines, for example.

The specific PEGylation of 3E8.scFv was investigated via a variant of 3E8.scFv called 3E8.scFv.Cys that contains a free cysteine at the C-terminus. In contrast to non-specific PEGylation in which numerous lysines were modified, specific PEGylation of

3E8.scFv.Cys results in the attachment of only one PEG molecule to a cysteine. This protein was modified with a 5 kD, 20 kD, 40 kD linear, and 40 kD branched PEG in order to comprehensively study the effects of specific PEGylation using molecules of different sizes and shapes. Characterization using gel filtration, differential scanning fluorimetry, and surface plasmon resonance showed that 3E8.scFv.Cys retained its monomeric state, stability, and binding affinity to TAG-72 after modification. Additional techniques such as multi-angle light scattering and small-angle X-ray scattering could provide more information on the shape of the PEG after conjugation and its interaction with the protein.

While PEGylated 3E8.scFv has the potential use as a tool in radioimmunoguided surgery, a variant of 3E8.scFv.FLAG was engineered to help pathologists analyze adenocarcinomas in vitro. Initial characterization showed that 3E8.scFv.FLAG binds just as well if not better to TAG-72 than first and second generation anti-TAG-72 antibodies like B72.3 and CC49. A scheme for immunohistochemistry using 3E8.scFv was developed and optimized using an anti-FLAG Biotin conjugate and streptavidin-horseradish peroxidase conjugate. The high potential of 3E8.scFv.FLAG as a selective and reliable tool for histological staining was confirmed using Western and dot blots that showed dark and immediate staining of the antigen and little to no background signal. Currently, 3E8.scFv.FLAG is being tested on human tissue arrays from various types of adenocarcinomas in different stages. The Magliery lab hopes that 3E8.scFv and its variants will improve the lives of cancer patients by allowing for the early detection and removal of tumors via immunohistochemistry and radioimmunoguided surgery, respectively.

References

1. "Leading Sites of New Cancer Cases and Deaths – 2015 Estimates." *Cancer Facts & Figures 2015*. American Cancer Society, n.d. Web. 20 Dec. 2015.
2. Sun, Duxin, et al. "Radioimmunoguided surgery (RIGS), PET/CT image-guided surgery, and fluorescence image-guided surgery: Past, present, and future." *Journal of surgical oncology* 96.4 (2007): 297-308.
3. Cohen, Alfred M., et al. "Radioimmunoguided surgery using iodine 125 B72. 3 in patients with colorectal cancer." *Archives of surgery* 126.3 (1991): 349-352.
4. Bertsch, David J., et al. "Radioimmunoguided surgery system improves survival for patients with recurrent colorectal cancer." *Surgery* 118.4 (1995): 634-639.
5. Martin, Daniel T., et al. "Intraoperative radioimmunodetection of colorectal tumor with a hand-held radiation detector." *The American Journal of Surgery*150.6 (1985): 672-675.
6. Xu, Mai, et al. "Expression of tag-72 in normal colon, transitional mucosa, and colon cancer." *International journal of cancer* 44.6 (1989): 985-989.
7. Arnold, MARK W., et al. "Intraoperative detection of colorectal cancer with radioimmunoguided surgery and CC49, a second-generation monoclonal antibody." *Annals of surgery* 216.6 (1992): 627.
8. Sickle-Santanello, Brenda J., et al. "Radioimmunoguided surgery using the monoclonal antibody B72. 3 in colorectal tumors." *Diseases of the Colon & Rectum* 30.10 (1987): 761-764.

9. Muraro, Raffaella, et al. "Generation and characterization of B72. 3 second generation monoclonal antibodies reactive with the tumor-associated glycoprotein 72 antigen." *Cancer research* 48.16 (1988): 4588-4596.
10. Kim, J. A., P. L. Triozzi, and E. W. Martin Jr. "Radioimmunoguided surgery for colorectal cancer." *Oncology (Williston Park, NY)* 7.2 (1993): 55-60.
11. Martin, Edward W., et al. "Radioimmunoguided surgery using monoclonal antibody." *The American journal of surgery* 156.5 (1988): 386-392.
12. Colcher, David, et al. "In vivo fate of monoclonal antibody B72. 3 in patients with colorectal cancer." *J Nucl Med* 31.7 (1990): 1133-1142.
13. Colcher, D., et al. "Monoclonal antibodies to human mammary carcinoma associated antigens and their potential uses for diagnosis, prognosis, and therapy." *Laboratory and research methods in biology and medicine* 8 (1983): 215.
14. Colcher, David, et al. "Differential binding to human mammary and nonmammary tumors of monoclonal antibodies reactive with carcinoembryonic antigen." *Cancer investigation* 1.2 (1983): 127-138.
15. Cote, Richard J., et al. "Intraoperative detection of occult colon cancer micrometastases using 125I-radiolabeled monoclonal antibody CC49."*Cancer* 77.4 (1996): 613-620.
16. Yoon, Sun Ok, et al. "Construction, affinity maturation, and biological characterization of an anti-tumor-associated glycoprotein-72 humanized antibody." *Journal of Biological Chemistry* 281.11 (2006): 6985-6992.
17. Wang, Wei, et al. "Antibody structure, instability, and formulation." *Journal of pharmaceutical sciences* 96.1 (2007): 1-26.

18. Ding, Haiming, et al. "Site Specific Discrete PEGylation of 124I-Labeled mCC49 Fab′ Fragments Improves Tumor MicroPET/CT Imaging in Mice."*Bioconjugate chemistry* 24.11 (2013): 1945-1954.
19. Jevševar, Simona, Menči Kunstelj, and Vladka Gaberc Porekar. "PEGylation of therapeutic proteins." *Biotechnology journal* 5.1 (2010): 113-128.
20. Roberts, M. J., M. D. Bentley, and J. M. Harris. "Chemistry for peptide and protein PEGylation." *Advanced drug delivery reviews* 64 (2012): 116-127.
21. Veronese, Francesco M., and Gianfranco Pasut. "PEGylation, successful approach to drug delivery." *Drug discovery today* 10.21 (2005): 1451-1458.
22. Fishburn, C. Simone. "The pharmacology of PEGylation: balancing PD with PK to generate novel therapeutics." *Journal of pharmaceutical sciences*97.10 (2008): 4167-4183.
23. Chapman, Andrew P. "PEGylated antibodies and antibody fragments for improved therapy: a review." *Advanced drug delivery reviews* 54.4 (2002): 531-545.
24. Niesen, Frank H., Helena Berglund, and Masoud Vedadi. "The use of differential scanning fluorimetry to detect ligand interactions that promote protein stability." *Nature protocols* 2.9 (2007): 2212-2221.
25. "Molecular Interaction Analysis, A Biacore Facility." *Molecular Interaction Analysis, A Biacore Facility*. Rutgers University School of Pharmacy, 19 Feb. 2005. Web. 24 Dec. 2015.
26. Pattnaik, Priyabrata. "Surface plasmon resonance." *Applied biochemistry and biotechnology* 126.2 (2005): 79-92.

27. Andrews, Ps. "Estimation of the molecular weights of proteins by Sephadex gel-filtration." *Biochemical Journal* 91.2 (1964): 222.
28. "Analytical Ultracentrifuge." *Institute Of Molecular Biophysics*. Florida State University. Web. 30 Dec. 2015.
29. Cole, James L., et al. "Analytical ultracentrifugation: sedimentation velocity and sedimentation equilibrium." *Methods in cell biology* 84 (2008): 143-179.
30. Alten, Edward D. "Improving Theranostic Proteins Through PEGylation: Cancer-Imaging Antibodies." Thesis. The Ohio State University, 2014. Print.
31. Epivatianos, A., et al. "Tumor-associated glycoprotein 72 (TAG-72) expression in salivary gland neoplasia: an immunohistochemical study using the monoclonal antibody (MAb) CC49." *Oral diseases* 6.2 (2000): 112-117.
32. Molinolo, Alfredo, et al. "Enhanced tumor binding using immunohistochemical analyses by second generation anti-tumor-associated glycoprotein 72 monoclonal antibodies versus monoclonal antibody B72. 3 in human tissue." *Cancer research* 50.4 (1990): 1291-1298.